Estimation of temporal and spatial variations in groundwater recharge in unconfined sand aquifers using Scots pine inventories

P. Ala-aho[1], P.M. Rossi[1] and B. Kløve[1]

[1] Water Resources and Environmental Engineering, Faculty of Technology, University of Oulu, P.O. Box 4300, 90014 University of Oulu, Finland

Correspondence to: P. Ala-aho (pertti.ala-aho@oulu.fi)

Abstract

Climate change and land use are rapidly changing the amount and temporal distribution of recharge in northern aquifers. This paper presents a novel method for distributing Monte Carlo simulations of 1-D soil profile spatially to estimate transient recharge in an unconfined esker aquifer. The modeling approach uses data-based estimates for the most important parameters controlling the total amount (canopy cover) and timing (depth of the unsaturated zone) of groundwater recharge. Scots pine canopy was parameterized to leaf area index (LAI) using forestry inventory data. Uncertainty in the parameters controlling soil hydraulic properties and evapotranspiration was carried over from the Monte Carlo runs to the final recharge estimates. Different mechanisms for lake, soil, and snow evaporation and transpiration were used in the model set-up. Finally, the model output was validated with independent recharge estimates using the water table fluctuation method and baseflow estimation. The results indicated that LAI is important in controlling total recharge amount, and the modeling approach successfully reduced model uncertainty by allocating the LAI parameter spatially in the model. Soil evaporation compensated for transpiration for areas with low LAI values, which may be significant in optimal management of forestry and recharge. Different forest management scenarios tested with the model showed differences in annual recharge of up to 100 mm. The uncertainty in recharge estimates arising from the simulation parameters was lower than the interannual variation caused by climate conditions. It proved important to take unsaturated depth and vegetation cover into account when estimating spatially and temporally distributed recharge in sandy unconfined aquifers.

1 Introduction

Eskers are permeable, unconfined sand and gravel aquifers (Banerjee, 1975). In addition to water supply, they support groundwater-dependent ecosystems and provide recreational services (Kløve et al., 2011). Esker hydrology is important as eskers and other glaciofluvial aquifer types cover large areas of the North and are among the dominant aquifer types in the boreal zone. Management of these complex aquifers has gained recent attention (Bolduc et al., 2005, Karjalainen et al., 2013, Koundouri et al., 2012, Kurki et al., 2013). The European Groundwater Directive requires such systems to be characterized in order to determine their quality status, so knowledge of how to estimate groundwater recharge is becoming increasingly important (EC, 2006). Esker aquifers are commonly covered with managed pine forests, where the forest canopy is likely to influence recharge amounts. The soil surface ~~profile~~ of eskers is complex and highly variable, consisting of kettle holes and sand dunes, resulting in variable depth of the unsaturated zone (Aartolahti, 1973), a factor which also needs to be accounted for in recharge estimation.

Computational methods to estimate groundwater recharge vary from simple water balance models, where water stores and fluxes are represented conceptually and related with adjustable parameters (Jyrkama et al., 2002), to physically-based models using the Richards equation (Assefa and Woodbury, 2013, Okkonen and Kløve, 2011) to solve water fluxes through unsaturated zone. Computational methods solving the Richards equation are often limited to small-scale areal simulations (Scanlon et al., 2002) and shallow unsaturated zones, and they commonly lack the soil freeze, thaw, and snow storage sub-routines relevant at higher northerly latitudes (Okkonen, 2011). However, computational approaches can be employed to produce the values on spatial and temporal variability in recharge often needed in groundwater modeling (Dripps and Bradbury, 2010). The methods developed so far commonly rely on a GIS platform for spatial representation and calculation approaches based on water balance to create the temporal dimension of recharge (Croteau et al., 2010, Dripps and Bradbury, 2007, Jyrkama et al., 2002, Sophocleous, 2000, Westenbroeck et al., 2010). Neglecting variations in depth of the unsaturated zone is common practice in many water balance models used in recharge estimations. However, the residence time in the unsaturated zone may play an important role, especially in the timing of recharge in deep unsaturated zones (Hunt et al., 2008), as acknowledged in recent work (Assefa and Woodbury, 2013, Jyrkama and Sykes, 2007, Scibek and Allen, 2006, Smerdon et al., 2008).

In numerical recharge models, actual evapotranspiration (ET) is a difficult variable to estimate accurately from climate, soil, and land use data. The vegetation is commonly parameterized from land use or land cover maps (Assefa and Woodbury, 2013, Jyrkama et al., 2002, Jyrkama and Sykes, 2007, Keese et al., 2005), where the vegetation characteristics and leaf area index (LAI) are estimated based solely on vegetation type. In addition to tree canopy transpiration, understorey evaporation can constitute a large proportion of total ET. Soil evaporation from the forest floor is generally reported to range from 3 to 40% of total ET (Kelliher et al., 1993), although values as high as 92% have been recorded (Kelliher et al., 1998). For conifer forest canopies, understorey evaporation can largely compensate for low transpiration in areas with lower LAI (Ohta et al., 2001, Vesala et al., 2005). Data on canopy-scale evaporation rates at latitudes above 60°N are rare (Kelliher et al., 1993). A few studies have estimated ET from pine tree stands at patch scale (Kelliher et al., 1998, Lindroth, 1985), but none has extended this analysis to spatially distributed groundwater recharge. Forest management practices have the potential to affect the transpiration characteristics of coniferous forests, which typically leads to increased groundwater recharge (Bent, 2001, Lagergren et al., 2008, Rothacher, 1970).

This study sought to expand the application of physically-based 1-D unsaturated water flow modeling to simulate spatial and temporal variations in groundwater recharge, while taking into account detailed information on vegetation (pine, lichen), unsaturated soil depth, cold climate, and simulation parameter uncertainty. CoupModel (Jansson and Karlberg, 2004) was used in simulations because of its ability to represent the full soil-plant-atmosphere continuum adequately and to include snow processes in the simulations (Okkonen and Kløve, 2011). The modeling set-up developed here uses spatially detailed information on tree canopy properties and concentrates on simulating different components of evapotranspiration. Furthermore, it considers the effect that forestry land use has on vegetation parameters and how this is reflected in groundwater recharge. The simulation approach takes into account the variability in the unsaturated depth throughout the model domain. Parameter uncertainty, often neglected in recharge simulations, is considered by using multiple random Monte Carlo simulation runs in the process of distributing the 1-D simulations spatially. The overall aim of the study was to provide novel information on groundwater recharge rates and factors contributing to the amount, timing, and uncertainty of groundwater recharge in unconfined sandy eskers aquifers.

2 Materials and Methods

2.1 Study site

Groundwater recharge was estimated for the case of the Rokua esker aquifer in northern Finland (Fig. 1). The climate at the Rokua aquifer is characterized by precipitation exceeding ~~evaporation~~ on an annual basis and statistics of the annual climate for the study period 1961 - 2010 in terms of precipitation, air temperature and FAO reference evapotranspiration according to Allen et al. (1998) is presented in Table 1. Another important feature of the climate is annually recurring winter periods when most precipitation is accumulated as snow. Groundwater recharge was estimated for a model domain of 82.3 km^2, 3.6 % of which is covered by lakes.

2.1.1 ~~Quantifying~~ Leaf area index from forestry inventories

Forestry inventory data from the Finnish Forest Administration (Metsähallitus, MH) and Finnish Forest Centre (Metsäkeskus, MK) were used to estimate LAI for the Rokua esker groundwater recharge area. The available data consisted of 2786 individual plots covering an area of 52.4 km^2 (62.4% of the model domain). The forestry inventories, performed mainly during 2000-2011, showed that Scots pine (*Pinus sylvestris*) is the dominant tree in the model area (94.2% of plots). The forest inventory data include a number of data attributes and the following data fields, included in both the MH and MK datasets, were used in the analysis:

- Plot area (p_A); [ha]
- Main canopy type
- Average tree stand height (h); [m]
- Average stand diameter at breast height (d_{bh}); [cm]
- Number of stems (n_{stm}); [1 ha^{-1}]
- Stand base area (b_A); [m^2 ha^{-1}]
- Stand total volume (V); [m^3]

Inventory plots were excluded from the analysis if: (1) main canopy type was not pine forest, (2) data were missing for d_{bh} and h or n_{stm}, or (3) the MH and MK datasets overlapped, in which case MH was retained. However, several plots in the MH dataset were lacking n_{stm}

data, which would have created a large gap in data coverage. Therefore the n_{stm} variable was estimated with a log-transformed regression equation using data on d_{bh} , p_A, and V as independent variables. This regression equation was built from 280 plots (R^2 = 0.88) and used to estimate n_{stm} for 288 plots. LAI was estimated as described by *Koivusalo et al.* (2008). Needle mass for an average tree in stand/plot was estimated from h and d_{bh} using empirical equations presented by Repola et al. (2007). LAI for a stand was calculated as:

$$LAI = Nm_t * n_{stm} * S_{LA} \quad (1)$$

where Nm_t = needle mass per average tree in stand [kg], n_{stm} = number of stems per hectare [1/ha], and S_{LA} = specific leaf area = 4.43 m^2 kg^{-1} = 4.43*10^{-4} ha kg^{-1} (Xiao et al., 2006).

~~Detailed information on LAI was used to obtain an estimate of how different land use management options, already actively in operation in the area, could potentially affect groundwater recharge.~~ Clear-cutting is an intensive land use form in which the entire tree stand is removed, and it is carried out in some parts of the study area. The first scenario simulated the impact of clear-cutting by not resorting to the estimated LAI pattern at the site (Fig. 2), but by using an LAI value of 0-0.2 ~~for the whole simulated area~~. In the second scenario, which was the opposite of clear-cutting, the mature stand was assumed to have high LAI values of 3.2-3.5 found at the study site and reported in the literature (Koivusalo et al., 2008, Rautiainen et al., 2012, Vincke and Thiry, 2008, Wang et al., 2004).

2.1.2 ~~Determination of lichen water retention in soil evaporation~~

An organic lichen layer covers much of the sandy soil at the Rokua study site (Kumpula et al., 2000), so this lichen layer was included in soil evaporation (SE) calculations. Lichen vegetation has the potential to affect SE by influencing the evaporation resistance of soil and by intercepting rainfall before it enters the mineral soil surface (Kelliher et al., 1998). Although lichens do not transpire water, their structural properties allow water storage in the lichen matrix and capillary water uptake from the soil (Blum, 1973, Larson, 1979). The lichen layer also increases soil surface roughness and thereby retards surface runoff (Rodríguez-Caballero et al., 2012).

In this study, water interception storage by the lichen layer was estimated from lichen samples. In total, six samples (species *Cladonia stellaris* and *C. rangiferina*) were taken in May 2011 from two locations 500 m apart, close to borehole MEA506 (see Fig. 1). These

samples were collected by pressing plastic cylinders (diameter 10.6 cm) through the lichen layer and extracting intact cores, after which mineral soil was carefully removed from the base of the sample. Thus the final sample consisted of a lichen layer on top and a layer of organic litter and decomposed lichen at the bottom, and was sealed in a plastic bag for transportation. To obtain estimates of water retention capacity, the samples were first wetted until saturation with a sprinkler, left overnight at +4 °C to allow gravitational drainage and weighed to determine 'field capacity'. The samples were then allowed to dry at room temperature and weighed daily until stable final weight ('dry weight') was reached. The water retention capacity (w_r) of the sample was calculated as:

$$w_r = \frac{m_{fc} - m_{dry}}{\rho_w} \cdot \frac{1}{\pi \cdot r^2} \quad (2)$$

where m_{fc} is the field capacity weight [M], m_{dry} is the final dry weight [M] at room temperature, ρ_w [M L^{-3}] is the density of water, and r [L] is the radius of the sampling cylinder.

The mean water retention capacity of the lichen samples was found to be 9.85 mm (standard deviation (SD) 2.71 mm) and approximations for these values were used in model parameterization (Table 2). In the simulations, the lichen layer was represented as an organic soil layer with similar Brooks and Corey parameterization as for mineral soil. To acknowledge the lack of information about Brooks and Corey parameter estimates for lichen, the parameters were included in the Monte Carlo runs (see section 2.2) with ranges which in our opinion produced reasonable shape of the pressure-saturation curve allowing easy drainage of the lichen.

2.1.3 ~~Geological data from soil samples~~

~~Particle size distribution~~ was determined from 26 soil samples taken from five boreholes at various depths (Fig. 1). 14 of the samples were analyzed also for pressure saturation curves. Samples were characterized as fine or medium sand, while soil ~~type~~ in the other boreholes (Fig. 1) had previously been characterized as medium, fine or silty sand throughout the model domain by the Finnish Environmental Administration. Therefore the soil samples from the five boreholes were considered to be representative of the soil type in the area. Pressure saturation data from the samples was then used to define parameter ranges for the Brooks and Corey equation used in the simulations (Table 2). Furthermore, ~~particle size distribution~~

values were employed to calculate the range of saturated vertical hydraulic conductivity for the samples, using empirical equations by Hazen, Kozeny-Carman, Breyer, Slitcher, and Terzaghi (Odong, 2007). The hydraulic conductivity for a given sample ranged approximately one order of magnitude between the equations. When using the five equations for the 26 samples in total, the calculated values were within $1.99*10^{-5}$ – $1.47*10^{-3}$ [m s^{-1}] for all but one sample. The obtained range was considered to reasonably represent the hydraulic conductivity variability in the study area and simulations (Table 2).

Water table was monitored for model validation purposes (Fig. 1) using pressure-based dataloggers (Solinst Levelogger Gold). A measurement was made at one-hour intervals in five boreholes screened 1-2 m below the water table. The depth of the unsaturated zone at these boreholes varied from 1 to 15 m. The data were used to estimate groundwater recharge with the water table fluctuation method (see section 2.5).

2.1.4 Climate data ~~to drive simulations~~

Driving climate data for the model were taken from Finnish Meteorological Institute databases for the modeling period 1 Jan 1961-31 Oct 2010. Daily mean temperature [°C] and sum of precipitation [mm] were recorded at Pelso climate station, 6 km south of the study area (Fig. 1). The most representative long-term global radiation data [kJ m^{-2} d^{-1}] for the area were available as interpolated values in a grid covering the whole of Finland. The interpolation data point was found to be at approximately the same location as borehole MEA2110 (Fig. 1). Long-term data on wind speed [m s^{-1}] and relative humidity [%] were taken from Oulunsalo and Kajaani airports, located 60 and 40 km from the study site, respectively. The data from the airports were instantaneous observations at three-hour intervals, from which daily mean values were calculated. All the climate variables were recorded at reference height 2 m except for wind speed, which was measured at 10 m height. The wind speed data were therefore recalculated to correspond to 2 m measurement height according *Allen et al.* (1998) by multiplying daily average wind speed by 0.748. The suitability of long-term climate data for the study site conditions was verified with observations made at a climate station established at the study site in an overlapping time period (Dec 2009-Oct 2010) and the agreement between the measurements was found to be satisfactory.

Data on long-term lake surface water temperature were needed to calculate lake evaporation (see section 2.3.3), but were not available directly at the study site. However, surface water temperature was recorded at Lake Oulujärvi by the Finnish environmental administration (2013) 22 km from the study site in the direction of the Kajaani climate station (Fig. 1). The Oulujärvi water temperature was found to be closely correlated (linear correlation coefficient 0.97) with daily lake water temperature recorded at Rokua during summer 2012. Daily lake surface temperature data for Lake Oulujärvi starting from 21 July 1970 were used in lake evaporation modeling. However, the data series had missing values for early spring and some gaps during five years in the observation period. These missing values were estimated with a sine function, corresponding to the average annual lake temperature cycle, and a daily time series was established for subsequent calculations.

~~It was essential to include snow accumulation in the simulations in order to represent the major spring recharge event of snowmelt. The snow accumulation routines in CoupModel were used (Jansson and Karlberg, 2004) and~~ snowmelt was calculated with a degree-day approach model. Snow routines were calibrated separately using bi-weekly snow water equivalent (SWE) data from Vaala snowline measurements (Finnish environment administration, 2011) for the period 1960-2010 (Fig. 1). This separately calibrated snow model was used for all subsequent simulations.

2.2 Modeling framework

Recharge was estimated by simulating water flow through an unsaturated one-dimensional (1-D) soil column with the Richards equation using CoupModel (Jansson and Karlberg, 2004). To distribute the simulations spatially, the recharge area was subdivided into different recharge zones, similarly to e.g. Jyrkämä et al. (2002). As each zone requires a unique simulation, the number of simulation setups rapidly increases, leading to high computational demand and/or laborious manual adjustment of model set-up. In the present study, this was avoided by simulating water flow in a single unsaturated 1-D soil column multiple times with different random parameterizations and distributing the results spatially to model zones. Spatial coupling was done with the ArcGIS software (ESRI, 2011).

Zonation in the model was based on two variables: LAI and unsaturated zone depth (UZD). The calculation of spatially distributed values for LAI and UZD is presented in detail in sections 2.1.1 and 2.4. This produced a grid map with 20m x 20m cell size with a floating

point number assigned to each cell, resulting in a total of 205 708 cells for the model domain. The spatially distributed data were then divided into 15 classes for LAI and 30 classes for UZD (Figs. 2 and 5). The classes are primarily equal intervals, which was convenient in the subsequent data processing, but in addition the frequency distributions of LAI and UZD cell values were used to assign narrower classes for parameter ranges with many values (see histograms in Figs. 2 and 5). Class interval for LAI was 0.2 units up to a value of 2 (class 1: LAI = 0-0.2, etc.) and 0.3 to the maximum LAI value of 3.5. Class interval for UZD was 1 m to 10 m depth and 2 m to the final depth of 51 m. Finally, the classified LAI and UZD data were combined to a raster map with 20m x 20m cell size, producing 449 different zones with unique combinations of LAI and UZD values.

Simulations for the unsaturated 1-D soil profile were made for the period 1970-2010, and before each run 10 years of data (1960-1970) were used to spin up the model. The time variable boundary condition for water flow at the top of the column was defined by driving climate variables and affected by sub-routines accounting for snow processes. All water at the top of the domain was assumed to be subjected to infiltration. This model simplification well is justified by the permeable soil type with high infiltration capacity (as noted by Keese et al., 2005). Deep percolation ~~as gravitational drainage~~ was allowed from soil column base using the unit-gradient boundary condition (see e.g. Scanlon et al., 2002). The column was vertically discretized into 60 layers with increasing layer thickness deeper in the profile: Layer thickness was 0.1 m until 1.6 m (the first layer lichen), 0.2 m between 1.6 and 3 m, 0.5 m between 3 and 10 m, 1 m between 10 and 17 m and 2 m from 17 m to the bottom of the profile (51 m).

The simulation was performed as 400 Monte Carlo runs to ensure enough model runs would be available for each LAI range. Model was ran each time with different parameter values as specified in Table 2. The parameters for which values were randomly varied were chosen beforehand by trial and error model runs exploring the sensitivity of parameters with respect to cumulative recharge or evapotranspiration. The parameter ranges were specified from field data when possible; otherwise we resorted to literature estimates or in some cases used ± 50% of the CoupModel default providing a typical parameter for the used equation.

Variation in the LAI and UZD parameters were used to allocate the simulations spatially to the study site. To follow the example in Figure 3, a cell with a LAI value of 0.1 was assigned to cell class 1 along with all other cells in the LAI range 0-0.2. In addition to LAI, the model

was zoned according to unsaturated zone depth. For each model cell, a value for simulated water flow was extracted from the midpoint of unsaturated soil class corresponding to the cell in question. In the example in Figure 3, a cell with an UZD value of 5.2 m belongs to soil class 6, representing unsaturated depth of 5-6 m. Water flow at 5.5 m depth represents the groundwater recharge time series for the model cell in question. In this way, each of the 400 simulations of the unsaturated soil column provided a water flow time series for each UZD class. When LAI class for the same example cell was considered, there were on average 27 simulation time series (number of total model runs [400] divided by number of LAI cell classes [15]) available for the example cell with UZD 5.2 m and LAI 0.15.

After completing the CoupModel simulations for the unsaturated soil column, each unique recharge zone (a combination of UZD and LAI class) had on average 27 recharge time series produced by different random combinations of parameters (Table 2). To propagate the variability in the 27 time series into the final areal recharge, a recharge value was randomly selected for each time step and each recharge zone from the ensemble of 27 (on average) and multiplied by the number of model cells belonging to the recharge zone in question (Eq. 3). Because the recharge rates were in units of mm/day, the rate was converted to volumetric flux [m^3 d^{-1}] by multiplying it by the cell area (A_c) with appropriate unit transformations. Finally, the volumetric flow rate from all the unique recharge zones was summarized for a given time step and the sum was converted from [m^3 d^{-1}] to [mm d^{-1}] by dividing by the surface area of the total recharge area (A_{tot}).This procedure was carried out for all time steps and then repeated a number of times (here 150 times) to ensure that all of the simulated time series for each recharge zone were represented in the random selection process.

$$R_{i,j} = \frac{\sum_{l=1}^{449} n(l) * Rs_{i,rand(1:k)} * A_c}{A_{tot}} \quad (3)$$

where $R_{i,j}$ is the final sample of areal recharge [mm day^{-1}], i is the index for simulation time step (= 1:14975), j is the index for sample for a given time step (1:150), l is the index for unique recharge zone, n(l) is the number of cells in a given recharge zone, Rs is the recharge sample [mm/day] for a given recharge zone at time step I, k is the number of time series for a given recharge zone, A_c is the surface area of a model raster cell (=20 m * 20 m = 400 m^2), and A_{tot} is the surface area of the total recharge area.

329 The resulting R matrix has 150 time series for areal recharge produced by simulations with
330 different parameter realizations. The variability between the time series provides an indication
331 of how much the simulated recharge varies due to different model parameter values. The
332 method allows computationally efficient recharge simulations, because the different recharge
333 zones do not all have to be simulated separately.

334 The method assumes that: (1) over the long-term, the water table remains at a constant level,
335 i.e. the unsaturated depth for each model cells stays the same. Monitoring data from 11
336 boreholes and seven lakes with more than 5 years of observation history shows level
337 variability of 1 – 1.5 m, with depressions and recoveries of the water table. This variability is
338 within the accuracy of water table estimation by interpolation, and therefore we find the
339 assumption of long term equilibrium acceptable for the study site. (2) the capillary fringe in
340 the sandy soil is thin enough not to affect the water flow before arriving at the 'imaginary'
341 water table at the center of each soil class. (3) only vertical flow takes place in the unsaturated
342 soil matrix, a typical assumption in recharge estimation techniques (Dripps and Bradbury,
343 2010, Jyrkama et al., 2002, Scanlon et al., 2002) (4) surface runoff is negligible primarily due
344 to the permeable soil type, and also due to lichen cover inhibiting runoff. The maximum
345 observed daily rainfall for the area has been 57.4 mm. Further assuming that rain for the day
346 fell only during one hour, it would equal to $1.59*10^{-5}$ m s^{-1} input rate of water, which is close
347 to the lower range of saturated hydraulic conductivity at the study site ($1.99*10^{-5}$ m s^{-1}).
348 Therefore rainstorms at the site very rarely exceed the theoretical infiltration capacity. As a
349 field verification, surface runoff has not been observed during field visits and the area lacks
350 intermittent or ephemeral stream networks. (5) uncertainties in the estimation of spatially
351 distributed LAI and UZD values justify the use of approximations (i.e. water flow at the UZD
352 class range midpoint and LAI value specified only as a range for each cell) in the cell
353 classification phase.

354 The model set-up used fine temporal and spatial discretization with a daily time step and 20m
355 x 20m cell size, respectively. The short time step was chosen to fully capture the main
356 recharge input from snowmelt and to demonstrate its impact on recharge variability at
357 different water table depths. The small model cell size was selected to ensure full exploitation
358 of the forest inventory plots in LAI determination. Simulation times for the current set-up
359 were approximately 10 hours for 400 simulations of the 50 m soil profile for the period 1961-
360 2010, and 12 hours to redistribute the simulations to the 200 000 model cells for each time

step and create 150 realizations of recharge time series. Where the computational capacity or the length of the run times poses a problem, the modeling methodology allows different spatial and temporal dimensions, which would speed up the long simulation times.

The sensitivity of the parameters varied in the simulations was tested with Kendall correlation analysis, by testing the correlation between each model parameter and cumulative sums of different evapotranspiration components and soil infiltration for the 400 model runs. Individual simulation with unique parameter values did not produce a groundwater recharge value due to the assembling strategy for recharge; therefore the ET components and soil infiltration were selected as variables for comparison. In addition, correlations were examined as scatter plots to ensure that possible sensitivity not captured by the monotonic correlation coefficient was not overlooked.

2.3 Estimation of Evapotranspiration

Four different evaporation processes were considered in this study; soil, snow, ~~and~~ lake evaporation and transpiration (Fig. 4). In areas with unsaturated soil zones, the first three evaporation components were estimated, along with water flow simulations, using CoupModel. However, as 3.6 % of the surface area of the study site consists of lakes (Fig. 1), lake evaporation from free water surfaces was calculated independently from the CoupModel simulations. Kettle hole lakes in esker aquifers often lack surface water inlets and outlets and are therefore an integral part of the groundwater system (Ala-aho et al., 2013, Winter et al., 1998), so we considered these lakes as contributors to total groundwater recharge. In other words, rainfall per lake surface area is treated equally as addition to the aquifer water storage as groundwater recharge. As a difference, lake water table is subjected to evaporation unlike the groundwater table.

2.3.1 Transpiration

Transpiration from the Scots pine canopy ($L_v E_{tp}$) was calculated using Penman-Monteith (P-M) combination Eq. (4):

$$L_v E_{tp} = \frac{\Delta R_n + \rho_a \cdot c_p \frac{(e_s - e_a)}{r_a}}{\Delta + \gamma\left(1 + \frac{r_s}{r_a}\right)} \quad (4)$$

where R_n is net radiation, ρ_a is air density, c_p is the specific heat of air, e_s is the vapor pressure at saturation, e_a is the actual air vapor pressure, r_a is the aerodynamic resistance, Δ is the slope of the saturated vapor pressure-temperature curve, γ is the psychrometer constant, and r_s is surface resistance.

The aerodynamic resistance (r_a) for transpiration was calculated as:

$$r_a = \frac{ln\left(\frac{z_{ref}-d}{z_0}\right)}{k^2 \cdot u} \quad (5)$$

where z_{ref} is the reference height of the measurements, d is the displacement height, z_0 is the roughness length, k is von Karman's constant, and u is wind speed.

Surface resistance (r_s) was estimated with Eq. 6:

$$r_s = \frac{1}{max(LAI \cdot g_l; 0.001)} \quad (6)$$

where g_l is the leaf conductance given by the Lohammar equation (see e.g. Lindroth, 1985).

Whenever possible, all the parameters relating to the Penman-Monteith equation were estimated based on data, namely LAI of the canopy. Surface resistance and saturation vapor pressure difference are the main factors controlling conifer forest evapotranspiration, while the aerodynamic resistance is of less importance (Lindroth, 1985, Ohta et al., 2001). In the calculation of aerodynamic resistance with the P-M equation, roughness length is related to LAI and canopy height, according to *Shaw and Pereira* (1982). Other parameters governing the aerodynamic resistance, except for LAI, were treated as constant. The surface resistance of the pine canopy was estimated with the Lohammar equation (see e.g. Lindroth, 1985), accounting for effects of solar radiation and air moisture deficit in tree canopy gas exchange. Because LAI values have a strong influence in the surface resistance Lohammar equation, the other parameters governing the surface resistance were excluded from the Monte Carlo runs. Distribution of root biomass with respect to depth from the soil surface was presented with an exponential function, because most Scots pine roots are concentrated in the shallow soil zone. A root depth of 1 m was used for the entire canopy (Kalliokoski, 2011, Kelliher et al., 1998, Vincke and Thiry, 2008).

2.3.2 Soil evaporation with lichen cover

Soil evaporation was calculated using an empirical approach (Eq. 7) based on the P-M equation, as described in detail in *Jansson and Karlberg* (2004). In this approach, soil evaporation ($L_v E_{tp}$) is calculated for the snow-free fraction of the soil surface, and the snow evaporation is solved separately as a part of snow pack water balance:

$$L_v E_{tp} = \frac{\Delta(R_n - q_h) + \rho_a \cdot c_p \frac{(e_s - e_a)}{r_{as}}}{\Delta + \gamma\left(1 + \frac{r_{ss}}{r_{as}}\right)} \quad (7)$$

where q_h is the soil surface heat flux, r_{as} is the aerodynamic resistance of soil, and r_{ss} is the surface resistance of soil.

The aerodynamic resistance of the soil (r_{as}) is calculated as Eq (8):

$$r_{as} = r_{alai} \cdot LAI + \frac{1}{k^2 \cdot u} \cdot ln\left(\frac{z_{ref} - d}{z_{0M}}\right) \cdot ln\left(\frac{z_{ref} - d}{z_{0H}}\right) \cdot f(R_{ib}) \quad (8)$$

where r_{alai} is an empirical parameter, z_{0M} and z_{0H} are surface roughness lengths for momentum and heat, respectively, and $f(R_{ib})$ is a function governing the influence of atmospheric stability.

The surface resistance for soil (r_{ss}) is given by:

$$r_{ss} = \begin{cases} r_\Psi \cdot log(\Psi_s - 1 - \delta_{surf}); & \Psi_s > 100 \\ r_\Psi(1 - \delta_{surf}); & \Psi_s \leq 100 \end{cases} \quad (9)$$

where r_Ψ is an empirical coefficient, Ψ_s is the water tension in the uppermost soil layer, and δ_{surf} is the mass balance at the soil surface (see Jansson and Karlberg, 2004).

In areas where the water table is close to the soil surface, the water table can provide an additional source of water for evapotranspiration (Smerdon et al., 2008). Simulations with a water table fixed at different depths in the soil profile would have been possible in the CoupModel setup. However, it would have doubled the amount of model runs for each considered water table depth and water table was not explicitly simulated for computational efficiency. Upward fluxes were not excluded from the recharge time series and negative fluxes were considered as “negative recharge” at any depth. Only the simplification is made

that water available for upward fluxes comes only ~~form~~ the soil moisture storage, not from the water table.

To take into account the decreased recharge for areas with near surface water tables, the recharge for cells with an unsaturated zone of <1 m was estimated with a water balance approach. We assumed that for areas with a shallow water table, soil water content was not a limiting factor for transpiration. Therefore an additional water source for transpiration was considered by making the transpiration rate equal to simulated potential transpiration (T) during times when the actual transpiration was simulated (T >0.05 mm). Increasing effect of the water table located at 1 m depth on soil evaporation was tested with simulations and found to be 5-10% higher with than without a water table. Therefore a 7% addition was made to the simulated actual soil evaporation for cells with a shallow water table. Daily recharge (R_{1m}, L T^{-1}) for cells with unsaturated depth below 1 m was estimated as:

$$R_{1m} = I - T_{adj} - ES_{adj} \qquad (10)$$

where I is infiltration water arriving to lake/soil surface, including both meltwater from the snowpack and precipitation [L T^{-1}] , T_{adj} [mm d^{-1}] is adjusted transpiration, and ES_{adj} [mm d^{-1}]is adjusted soil evaporation.

2.3.3 Lake evaporation

Lake cells were identified according from a base map and the daily lake recharge (R_{lake}, [L T^{-1}]) per unit area was then calculated with a water balance approach as:

$$R_{lake} = I - E_{lake} \qquad (11)$$

where E_{lake} [L T^{-1}] is lake evaporation.

Lake evaporation (E_{lake}) was estimated with the mass transfer approach (see e.g. Dingman, 2008) according to Eq. (12).

$$E_{lake} = K_E \cdot v_a \cdot (e_s - e_a) \qquad (12)$$

where K_E is mass transfer coefficient [$ML^{-1}T^{-2}$], v_a is wind speed [L T^{-1}], e_s [$ML^{-1}T^{-2}$] is saturated vapor pressure at lake water surface temperature, and e_a [$ML^{-1}T^{-2}$] is air vapor pressure. The mass transfer coefficient (K_E) represents the efficiency of vertical water transport from the evaporating surface and it can be treated as a function of lake size:

$$K_E = 1.69 \times 10^{-5} \cdot A_L^{-0.05} \quad (13)$$

where A_L is lake surface area [km^2]

The groundwater recharge study area has lakes of variable size, from less than 1 ha to 25 ha (Fig. 1). Lake size variability was included in the total recharge calculation by randomly selecting a K_E value (from the range 1-25 ha) in Eq. (13) when calculating lake evaporation, and thereby groundwater recharge in model cells with lakes (see section 2.2). The mass transfer method was selected because of its simplicity, daily output resolution, low data requirement, and physically-based approach. However various calculation methods could easily be used in the modelling framework, depending on the data availability (see e.g. Rosenberry et al., 2007). If lake percentage in the area of interest is high, more sophisticated methods may be required to better represent the system. However, for the Rokua site the bias introduced by a simplistic approach was considered minor.

2.4 Estimation of unsaturated layer depth

The depth of the unsaturated layer at each model cell was estimated by subtracting interpolated water table level from digital elevation model (DEM) topography calculated based on LiDAR data (*National land survey of Finland*, 2012). The water table elevation was estimated with the ordinary Kriging interpolation method from four types of observations: water table boreholes, stages of kettle hole lakes, elevation of wetlands located in landscape depressions, and land surface elevation at the model domain (Fig. 5).

Water table borehole observations give the most accurate and reliable estimate of the water table position because they provide direct measurements on the water table. The water table elevation in a given piezometer was estimated here as the average value of the entire measurement history of each piezometer.

Kettle hole lakes in the area are imbedded in the aquifer and thus reflect the level of the regional water table (Ala-aho et al., 2013). The lake stage was extracted as the DEM elevation for a given lake, while for large lakes several interpolation points were scattered around the lake shore to better steer the interpolation locally.

Wetland elevation was used as a proxy for the water table elevation in locations where more certain observations (piezometers, lake levels) were lacking. If a wetland was present in the topographical depression, the water table was considered to lie at the depression bottom, in

order to sustain the conditions needed for wetland formation. Wetlands were detected from the base map and the value for water table proxy was assigned from the DEM.

Finally, the land surface elevation was considered to give a reasonable estimate of the water table position in the transition zone between recharge and discharge areas. The Rokua aquifer is phreatic in the recharge area and Rossi et al. (2012) demonstrated that the peatlands partially confine the aquifer and can create artesian conditions in the discharge area. Even though some local overestimation of the water table may have resulted from the approximation method at the transition zone, it was found to be important to have some points to guide the interpolation at the model domain boundary in order to acknowledge the characteristics of the sloping water table towards the discharge area. The proxy used for water table was extracted from the DEM to points approximately 250 m apart at the boundary of the model domain.

2.5 Model validation

Model performance was tested by comparing the simulated recharge values with two independent recharge estimates in local and regional scale; the water table fluctuation (WTF) method and base flow estimation, respectively. The WTF method is routinely used to estimate groundwater recharge because of its simplicity and ease of use, and assumes that any rise in water level in an unconfined aquifer is caused by recharge arriving at the water table. For a detailed description of the method and its limitations, see e.g. Healy and Cook (2002). The recharge amount (R, L T^{-1}) is calculated based on the water level prior to and after the recharge event and the specific yield of the soil:

$$R = S_y \frac{\Delta h}{\Delta t} \qquad (14)$$

where S_y is the specific yield, h is the water table height [L], and t is the time of water table rise [T].

The WTF method requires groundwater level data with adequate resolution for both time and water level, to identify periods of rising and falling water table. Such data, with hourly interval water level recordings were available for the study site from six water table wells with average unsaturated zone depths of 1.2, 1.6, 5.0, 8.0, 9.3, and 14.7 m (Fig. 1). Wells where the water table was <2 m from the ground surface responded to major precipitation events. In the deeper wells, only the recharge from snowmelt was seen as water table rise.

Estimates of the soil specific yield are required for the calculations (Eq. 14), but no soil samples were available from the wells used in water table monitoring. Drilling records for these wells reported fine and medium sand, which was consistent with the particle size distribution for other wells in the area. Therefore an estimated value of 0.20-0.25 for the specific yield of all wells was used, according to typical values for fine and medium sand (Johnson, 1967).

The recharge estimated with the WTF method was compared with the simulated recharge during the recorded water level rise in the well. For each well, the cumulative ~~sum~~ of simulated water flow was extracted from soil profile depth corresponding to well water table depth. As an example, the simulated recharge in well ROK1 (unsaturated depth on average 14.7 m) was extracted from soil class 12, corresponding to recharge for unsaturated thickness of 14-16 m. All 400 model runs were used, providing 400 estimates for recharge for each time period of recorded water level rise.

A regional estimate of groundwater recharge was estimated as baseflow of streams originating at the groundwater discharge area. Because the Rokua esker aquifer acts as a regional water divide, stream flow was monitored around the esker, in total of 18 locations (Fig. 1). The flows were measured total of 8 times between 6 July 2009 and 3 August 2010 (see Rossi et al., 2014). The lowest total outflow during 9-10 February 2010 was recorded after three months of snow cover period, when water contribution to streams from surface runoff was minimal. The minimum outflow was considered as baseflow from the aquifer reflecting long term groundwater recharge in the area. However, some groundwater discharges to larger regional lakes and rivers traveling underneath the measured small streams (Rossi et al., 2014), and thereby the baseflow to the small streams was expected to be lower than the total recharge.

3 Results

3.1 Model validation with the WTF and baseflow methods

The model showed reasonable performance and consistency against independent recharge estimates obtained with both WTF and baseflow methods (Fig. 6 and Table 3, respectively). The WTF method agreed well with the simulated values, with overlapping estimates between the methods for all but two boreholes. Also the median value of simulations was close to WTF method, with some bias to higher estimates from the simulations. The order of magnitude for regional estimate of recharge, stream baseflow, corresponded well to simulated recharge, level of match depending on the examined simulation period (Table 3). The measured baseflow was 70 500 m^3 s^{-1}, or 312.7 mm a^{-1} when related to the recharge area. When comparing to the simulated long term average recharge and recharge for previous year, the measured baseflow was lower than the simulated recharge. Then again, when extracting the recharge data for the exact stream discharge measurements dates 9-10 February 2010, stream baseflow exceeded the simulated recharge.

3.2 Recharge and evapotranspiration time series

The dynamics of water flow time series responded to snowmelt and rain storm events rapidly at 1.5 m depth, but because of permeable sandy soils a clear signal of annual snowmelt was evident throughout the depth of the aquifer (Fig. 7). The data showed a delay in response to wet seasons when moving down in the soil profile, as expected. For example, snowmelt in the beginning of May 2008, gave the highest flow rate at 11 m in 19 May 2008, at 23 m in 29 June 2008 and at 49 m in 5 April 2009. Temporal variability is pronounced higher in the soil profile showing larger variability between maximimum and minimum flow.

Average land surface ET components remained relatively constant between years, but the simulated ET displayed a wide spread between simulations (Fig. 8). Estimated ~~evaporation~~ from the land surface (mean 237.6 mm) was somewhat lower than previous regional estimates of total ET (300 mm; (Mustonen, 1986)). Lake evaporation rates were generally higher than evapotranspiration from the land surface due to the different method for estimating lake evaporation. The variation in simulated lake evaporation was considerably lower than that in ET, as a different approach was used to account for uncertainty in the simulations.

Transpiration showed greater variation between simulations than soil evaporation and total land surface ET. On average, transpiration also comprised a slightly larger share of total evaporation than soil evaporation. Simulated snow evaporation was a small, yet not insignificant, component in the total ET from land surface.

When recharge simulation time series were summarized to annual values (1 Oct-30 Sept), recharge rates co-varied with annual infiltration (Fig. 9). Both annual recharge and infiltration displayed an increasing trend. The plot also showed the level of uncertainty in annual recharge values introduced by differences in model parameterization (see Table 2). The difference between minimum and maximum value for simulated annual recharge was on average 23.0 mm. Thus the maximum variablity in recharge estimates was 6.3 % of mean annual recharge 362.8 mm.

Annual recharge was strongly correlated with annual sum of precipitation (linear correlation coefficient 0.89) as expected based on previous work in humid climate and sandy soils (Keese et al., 2005, Lemmelä, 1990). According to the simulations, the *effective rainfall*, i.e. the percentage of corrected rainfall resulting in groundwater recharge annually, was on average 59.3%. This is in agreement with previous studies on unconfined esker aquifers at northerly latitudes, in which the proportion of annual precipitation percolating to recharge is reported to be 50-70% (71% by Zaitsoff (1984), 54% by Lemmelä and Tattari (1986) and 56% by Lemmelä (1990)). The percentage of effective rainfall varied considerably~~, by almost 30 %-units,~~ between different hydrological years, from 44.8% in some years up to 73.1% in others. Tests on whether the interannual variation in effective rainfall percentage could be explained by sum of annual precipitation or maximum snow water equivalent showed no correlation between either of these variables and effective recharge coefficient for a given year.

3.3 Spatial distribution of groundwater recharge

The spatial distribution of groundwater recharge was mostly due to variations in LAI originating from forestry data, distance to water table, and distribution of lakes (Fig. 10). Higher evaporation rates from lakes led to lower recharge in lakes (see red spots in Fig. 10). Similarly, large LAI led to high ET and resulted in low recharge in plots with high LAI. Other areas of low recharge, although not as obvious at the larger spatial scales shown in Fig. 10, were cells with a shallow water table (section 2.3.2). The effect of high ET at locations with a shallow water table can best be seen in south-east parts of the aquifer.

3.4 Influence of simulation parameters on groundwater recharge

Kendall correlation analysis of simulation parameters and annual average model outputs identified LAI as the most important parameter controlling evapotranspiration and infiltration (Table 4). Parameters related to soil hydraulics and evaporation showed some sensitivity to simulation results, while the parameters for lichen vegetation were only slightly sensitive or insensitive to simulation output variables.

The LAI parameter governed the level of evaporation for different ET components (Fig. 11). Evaporation from soil (and snow) compensated for mean annual ET for LAI values up to around 1.0, after which total ET increased as a function of LAI.

The scenarios for low (0 … 0.2) and high (3.2 … 3.5) LAI would change the groundwater recharge rates compared to the current LAI distribution (Fig. 9). In the high LAI scenario the annual recharge was on average 101.7 mm lower than in the low LAI situation. These results suggest that management of the Scots pine canopy has a significant control on the total recharge rates in unconfined esker aquifers.

4 Discussion

The modeling approach developed here used forestry inventory data to simulate spatial and temporal variations in recharge. The Richards equation-based 1-D simulations were spatially distributed using Monte Carlo runs for an unsaturated soil column. Within the Monte Carlo process, residence time in the unsaturated zone was accounted for, while uncertainty in selected model parameters was propagated to the final recharge time series.

Model validation showed that the modeling approach could reasonably reproduce (1) the main groundwater recharge events when compared to the WTF method and (2) the regional level of recharge compared to stream baseflow. The WTF estimates for recharge agreed with the simulations, with a slight tendency for higher estimates by the simulations. The discrepancy can be due to different assumptions behind the methods and uncertainty in local parameterization; in the WTF method for the specific yield and for simulations mainly the hydraulic conductivity which dictates the timing of recharge. However, there were overlapping estimates for almost every recharge event which shows consistency between the methods. The stream baseflow was lower than the long term average recharge, which was expected because of the site hydrogeology. All of the outflow from the aquifer was likely not

captured by the baseflow measurements as some of the water discharges to larger streams and lakes outside of the stream catchments (Rossi et al., 2014). When simulated recharge was extracted specifically for the baseflow measurements dates, the lower values for simulated recharge were also anticipated. The recharge displayed strong seasonal variability (see Fig. 7), but the discharge to streams is in general more stable because of the stabilizing effect of the groundwater storage. In conclusion, the order of magnitudes in the regional baseflow estimate and the simulation results were consistent. ~~Despite the very different assumptions on which the modelling and field based methods were based, all provided similar estimates for groundwater recharge at the study site.~~

There were different water flow rates at different depths (Fig. 7), demonstrating the role of the unsaturated zone in recharge. The high fluctuation in water flow at 1.5 m revealed the recharge dynamics in aquifers with a shallow water table. Such aquifers would be highly sensitive to annual fluctuations in recharge and respond rapidly to dry periods. On the other hand, rainy years would most likely replenish the aquifer water stores very quickly. Deeper in the soil profile, the response to wet and dry seasons was more modest, but still exhibited a clear seasonal signal. The water flow appeared to have dry and wet cycles of 5-10 years. Considering this, aquifers with unsaturated zones measuring tens of meters are likely to respond only to wet and dry cycles in climate patterns, rather than the weather in individual years. The temporal availability of the groundwater resource is most likely different for aquifers with different unsaturated zone geometry, as suggested by e.g. Hunt et al. (2008) and Smerdon et al. (2008).

According to the simulations, the percentage of precipitation forming groundwater recharge varied considerably between years, as also reported in previous studies on transient recharge (Assefa and Woodbury, 2013, Dripps and Bradbury, 2010). Even though annual recharge was correlated with annual precipitation, and therefore years with high precipitation resulted in higher absolute recharge (Fig. 9), the percentage of effective rainfall did not increase as a function of annual sum of precipitation. This is somewhat surprising, because the rather constant evaporation potential between years (Fig. 8) and high soil hydraulic conductivity could be expected to result in a higher percentage of rainfall reaching the water table in rainy years. Some studies (Dripps and Bradbury, 2010, Okkonen and Kløve, 2010) have suggested that when the main annual water input arrives as snowmelt during the low evaporation season, it is likely to result in higher percentage recharge than in a year with little snow storage and

precipitation distributed evenly throughout summer and autumn, which may contribute to the variability in the recharge coefficient. However, when the maximum annual SWE value was used as a proxy for annual snowfall, there was no evidence of snow amount explaining the interannual variability in the recharge coefficient. Other factors contributing to recharge coefficient variability may be related to soil moisture conditions prior to snowfall, or the intensity of summer precipitation events (Smerdon et al., 2008, Stähli et al., 1999). Furthermore, the variability can to some extent be an effect of annual summation for the period 1 Oct-30 Sept, usually considered the hydrological year in the Nordic climate. Therefore the rainy autumn season is cut in 'half', and because recharge event comes with some delay from precipitation, the rainfall considered for a given year may not be reflected in the recharge for the year.

The above-mentioned reasons make the concept of effective rainfall, which is currently routinely used to estimate groundwater recharge for groundwater management in e.g. Finland (Britschgi et al., 2009), susceptible to over- or under-estimation of actual annual recharge. This applies especially for aquifers with a thick unsaturated zone, where rainy years produce higher average recharge with some delay and for a longer duration (see Fig. 7). Therefore, if allocated water abstraction permits e.g. 50% effective rainfall coefficient to be assumed for each year, it potentially allows overuse of the resource during dry seasons. While aquifer storage can buffer occasional over-extraction, the lowering of the water table may diminish groundwater discharge to surface water bodies, depending on the geometry of the aquifer (Zhou, 2009).

The method used here to estimate LAI from forestry inventories introduces a new approach for incorporating large spatial coverage of detailed conifer canopy data into groundwater recharge estimations. LAI values reported for conifer forests in Nordic conditions similar to the study site are in the range 1-3, depending on canopy density and other attributes (Koivusalo et al., 2008, Rautiainen et al., 2012, Vincke and Thiry, 2008, Wang et al., 2004). The LAI values obtained for the study site (mean 1.25) were at the lower end of this range. Furthermore, the data showed a bimodal distribution, with many model cells with low LAI (< 0.4) lowering the mean LAI. The low LAI values were not considered to be an error in data or calculations, but were in fact expected because of active logging and clearcutting activities in the study area. Although the equations to estimate LAI are empirical in nature and based on simplified assumptions, the method can outline spatial differences in canopy structure.

However, the LAI estimation method could be further validated with field measurements or Lidar techniques (Chasmer et al., 2012, Riaño et al., 2004).

Plant cover, represented as LAI, proved to be the most important model parameter determining the total recharge amount. This has been reported in earlier studies estimating groundwater recharge (Dripps, 2012, Keese et al., 2005, Sophocleous, 2000), but here the vegetation was represented with more spatially detailed patterns and a field data-based approach for LAI. According to previous studies, average ET from boreal conifer forests is around 2 mm d^{-1} during the growing season (Kelliher et al., 1998) , which is ~~in~~ similar to our average value of 1.6 mm d^{-1} for the period 1 May-31 Oct. Some earlier studies have claimed that the influence of LAI on total ET rates from boreal conifer canopies is minor (Kelliher et al., 1993, Ohta et al., 2001, Vesala et al., 2005), but our simulation results indicate that higher LAI values lead to higher total ET values. While soil evaporation partly compensated for the lower transpiration with low LAI values, the total annual ET values progressively increased as a function of LAI (Fig. 11). Interestingly, the simulations suggested that ET remains constant in the LAI range 0-1, potentially due to the sparse canopy changing the aerodynamic resistance and partitioning of radiation limiting soil evaporation, while still not contributing much to transpiration in total ET. This suggests that the maximum groundwater recharge for boreal Scots pine remains rather constant up to a threshold LAI value of around 1. This knowledge can be used when co-managing forest and groundwater resources in order to optimize both.

The method allowed different land use scenarios in forestry management to be tested. The simulations showed that variable intensity of forestry, from low canopy coverage (LAI = 0-0.2) to dense coverage (LAI = 3.2-3.5) resulted in a difference of over 100 mm in annual recharge (Fig. 9). It can be argued that the scenarios are unrealistic, because high LAI values, covering the whole study site, may not be achieved even with a complete absence of forestry operations. Nevertheless, the result demonstrates a substantial impact of forestry operations on esker aquifer groundwater resources. Wider use of this method in Finland is practically possible, as active forestry operations in Finland have yielded an extensive database on canopy coverage, which could be used in groundwater management.

The lichen layer covering the soil surface was explicitly accounted for in the simulation set-up, which to our knowledge is a novel modification. *Kelliher et al.* (1998) concluded that precipitation intercepted by lichen was an important source of understorey evaporation,

especially directly after rain events. In addition, Bello and Arama (1989) reported that lichen could intercept light rain showers completely and that only intense rain events caused drainage from lichen canopy to mineral soil. While the lichen layer might have an increasing effect on soil evaporation through 'interception storage', Fitzjarrald and Moore (1992) suggest that a lichen cover may in fact have an insulating influence on heat and vapor exchange between soil and atmosphere, therefore impeding evaporation from the mineral soil. In the present study, the lichen layer appeared to have minor influence on total evaporation, soil evaporation and infiltration, as these variables showed some sensitivity to lichen Brooks and Corey parameters (Table 4). However, more intensive laboratory measurement of lichen water retention and conduction properties is required to clarify the role of lichen in soil evaporation, and thereby groundwater recharge.

Stochastic variation of selected model parameters illustrated the uncertainties relating to numerical recharge estimation using the Richards equation in one dimension. The capability and robustness of the Richards equation to reproduce soil water content and water fluxes have been demonstrated extensively in various studies (Assefa and Woodbury, 2013, Scanlon et al., 2002, Stähli et al., 1999, Wierenga et al., 1991). However, we considered that model calibration and validation with point observations of variables such as soil volumetric water content or soil temperature would not provide novel insights into water flow in unsaturated soils. Instead, we incorporated the parameter uncertainty ranges, usually used in model calibration, to the final recharge simulation output. An important outcome was that the uncertainty in the model output caused by different model parameterizations was small in comparison with the interannual variation in recharge. The error caused by uncertainty in the model assumptions or driving climate data was not addressed in this study. We presume that for the given case study, the uncertainty and suitability of the driving climate data would introduce more uncertainty into the model output than model parameterization.

~~While it can be argued that all relevant parameters were not included and parameter ranges could be more carefully determined,~~ the parameter set used was able to provide information on parameter sensitivity. LAI was the most important parameters controlling total ET, and thereby the amount of groundwater recharge (Table 4, Fig. 11). The LAI parameter was included in the equations controlling both transpiration and soil evaporation, and therefore the sensitivity of the parameter is not surprising. However, LAI is a measurable parameter in the otherwise semi-empirical equations used to simulate evaporation, and physically-based

parameters are preferable to empirical-fitting parameters in deterministic simulation approaches. Thus the ability of the approach to reduce a large part of model variability by allocating the LAI parameter spatially is a substantial advantage in reducing the model uncertainty.

The sensitivity analysis performed focused on total cumulative values of ~~flux variables~~ and did not address the temporal variations in the variables. Therefore the soil hydraulic parameters showed only minor sensitivity, perhaps misleadingly. Soil hydraulic parameters mainly influenced the timing of recharge through residence time in the soil, not so much the total amount. It should be noted that vertical heterogeneity in the soil profile hydraulic parameters can reduce the total recharge rates (Keese et al., 2005). However, vertical heterogeneities were ignored in this study not only to simplify the model, but also because the drilling logs showed only little variation in the area. Work of Wierenga et al. (1991) supports the simplification by showing that excluding moderate vertical heterogeneities does not significantly affect the performance of water flow simulations with the Richards equation. Spatial differences in hydraulic parameters could be more accurately implemented in the modeling approach by creating a third zonation based on soil type, in addition to LAI and UZD. This would require the parameter ranges for hydraulic conductivity and Brooks and Corey parameters to be expanded to cover the properties of different soil types. Even then, the model is applicable only in situations where the soil type is permeable enough to allow rapid infiltration, so that surface runoff can be assumed to be of minor importance.

5 Conclusions

A physically-based approach to simulate groundwater recharge for sandy unconfined aquifers in cold climates was developed. The method accounts for the influence of vegetation, unsaturated zone depth, presence of lakes, and uncertainty in simulation parameters in the recharge estimate. It is capable of producing spatially and temporally distributed groundwater recharge values with uncertainty margins, which are generally lacking in recharge estimates, despite understanding of uncertainty related to recharge estimates being potentially crucial for groundwater resource management. However, the parameter uncertainty defined for the study area was of minor significance compared with interannual variations in the recharge rates introduced by climate variations. The uncertainty caused by model parameterization was decreased by allocating the LAI parameter spatially in the model area.

The simulations showed that Scots pine canopy, parameterized as leaf area index (LAI), was important in controlling the total amount of groundwater recharge. Forestry inventory databases were used to estimate and spatially allocate the LAI and the results showed that such inventories could be better utilized in groundwater resource management. A sensitivity analysis on the parameters used showed that understorey evaporation could compensate for low LAI-related transpiration up to a LAI value of approximately 1, which may be important in finding the optimal level for forest management in groundwater resource areas. The concept of effective rainfall gave inconsistent estimates of recharge in annual timescales, showing the importance of using physically-based recharge estimation methods for sustainable groundwater recharge management.

Author contribution

P. Ala-aho and P.M Rossi collected and analyzed the field data. P.Ala-aho designed the simulation set-up, performed the simulations and interpreted the results. P.Ala-aho prepared the manuscript with contributions from all co-authors.

Acknowledgements

This study was made possible by the funding from EU 7th Framework programme GENESIS (Contract Number 226536), Academy of Finland AKVA research program, the Renlund Foundation, VALUE doctoral school and Maa- ja vesitekniikantuki ry. We would like to express our gratitude to Geological survey of Finland, Finnish Forest Administration (Metsähallitus) and Finnish Forest Centre (Metsäkeskus), Finnish meteorological institute, Finnish environmental admisitration and National land survey of Finland for providing datasets and expert knowledge that made this study possible in its current extent. To reproduce the research in the paper, data from above mentioned agencies can be made available for purchase on request from the corresponding agency, other data can be provided by the corresponding author upon request.

References

Aartolahti, T.: Morphology, vegetation and development of Rokuanvaara, an esker and dune complex in Finland, Societas geographica Fenniae, Helsinki, 1973.

Ala-aho, P., Rossi, P. M. and Kløve, B.: Interaction of esker groundwater with headwater lakes and streams, J. Hydrol., 500, 144-156, doi:10.1016/j.jhydrol.2013.07.014, 2013.

Allen, R., Pereira, L., Raes, D. and Smith, M.: Crop evapotranspiration - Guidelines for computing crop water requirements, Food and Agriculture Organization of the United Nations, Rome, 1998.

Assefa, K. A. and Woodbury, A. D.: Transient, spatially- varied groundwater recharge modelling, Water Resour. Res., 49, 1-14, doi:10.1002/wrcr.20332, 2013.

Banerjee, I.: Nature of esker sedimentation, in: Glaciofluvial and glaciolacustrine sedimentation, Jopling, A. V. and McDonald, B. C. (Eds.), Soc. Econ. Paleontol. Mineral., Special Publication 24, 1975.

Bello, R. and Arama, A.: Rainfall interception in lichen canopies, Climatol. Bull, 23, 74-78, 1989.

Bent, G. C.: Effects of forest-management activities on runoff components and ground-water recharge to Quabbin Reservoir, central Massachusetts, For. Ecol. Manage., 143, 115-129, 2001.

Blum, O. B.: Water relations, in: The lichens, Ahmadjian, V. and Hale, M. E. (Eds.), Academic Press Inc., USA, 381-397, 1973.

Bolduc, A., Paradis, S. J., Riverin, M., Lefebvre, R. and Michaud, Y.: A 3D esker geomodel for groundwater research: the case of the Saint-Mathieu–Berry esker, Abitibi, Quebec, Canada, in: Three-Dimensional Geologic Mapping for Groundwater Applications: workshop extended abstracts, Salt Lake City, Utah, 15 Oct, 2005.

Britschgi, R., Antikainen, M., Ekholm-Peltonen, M., Hyvärinen, V., Nylander, E., Siiro, P. and Suomela, T.: Mapping and classification of groundwater areas, The Finnish Environment Institute, Sastamala, Finland, 75 pp., 2009.

Chasmer, L., Pertrone, R., Brown, S., Hopkinson, C., Mendoza, C., Diiwu, J., Quinton, W. and Devito, K.: Sensitivity of modelled evapotranspiration to canopy characteristics within the Western Boreal Plain, Alberta, in: Remote Sensing and Hydrology, Proceedings of a Symposiom at Jackson Hole, Wyoming, USA, September 2010, 2012.

Croteau, A., Nastev, M. and Lefebvre, R.: Groundwater recharge assessment in the Chateauguay River watershed, Canadian Water Resources Journal, 35, 451-468, 2010.

Dingman, S. L.: Physical hydrology, Waveland Press Inc, Long Grove, IL, 2008.

869 Dripps, W.: An Integrated Field Assessment of Groundwater Recharge, Open Hydrology
870 Journal, 6, 15-22, 2012.

871 Dripps, W. and Bradbury, K.: The spatial and temporal variability of groundwater recharge in
872 a forested basin in northern Wisconsin, Hydrol. Process., 24, 383-392, doi:10.1002/hyp.7497,
873 2010.

874 Dripps, W. and Bradbury, K.: A simple daily soil–water balance model for estimating the
875 spatial and temporal distribution of groundwater recharge in temperate humid areas,
876 Hydrogeol. J., 15, 433-444, doi:10.1007/s10040-007-0160-6, 2007.

877 EC: Directive 2006/118/EC of the European Parliament and of the Council on the protection
878 of groundwater against pollution and deterioration, 2006.

879 ESRI: ArcGIS Desktop: Release 10, Environmental Systems research institute, Redlands,
880 Texas, 2011.

881 Finnish environmental administration: Oiva – the environmental and geographical
882 information service. Observation station number 5903320. Data extracted 27 June 2013,
883 2013.

884 Finnish environmental administration: Oiva – the environmental and geographical
885 information service. Observation station number 1592101. Data extracted 11 Feb 2011, 2011.

886 Fitzjarrald, D. R. and Moore, K. E.: Turbulent transports over tundra, J. Geophys. Res., 97,
887 16717-16729, 1992.

888 Healy, R. W. and Cook, P. G.: Using groundwater levels to estimate recharge, Hydrogeol. J.,
889 10, 91-109, 2002.

890 Hunt, R. J., Prudic, D. E., Walker, J. F. and Anderson, M. P.: Importance of unsaturated zone
891 flow for simulating recharge in a humid climate, Ground Water, 46, 551-560, 2008.

892 Jansson, P. and Karlberg, L.: Coupled heat and mass transfer model for soil-plant-atmosphere
893 systems, Royal Institute of Technolgy, Dept of Civl and Environmental Engineering,
894 Stockholm, 435 pp., 2004.

895 Johnson, A. I.: Specific yield: compilation of specific yields for various materials, US
896 Government Printing Office, Washington, 1967.

897 Jyrkama, M. I. and Sykes, J. F.: The impact of climate change on spatially varying
898 groundwater recharge in the grand river watershed (Ontario), J. Hydrol., 338, 237-250, 2007.

899 Jyrkama, M. I., Sykes, J. F. and Normani, S. D.: Recharge estimation for transient ground
900 water modeling, Ground Water, 40, 638-648, 2002.

901 Kalliokoski, T.: Root system traits of Norway spruce, Scots pine, and silver birch in mixed
902 boreal forests: an analysis of root architecture, morphology, and anatomy, Ph.D. thesis,

903 Department of Forest Sciences, Faculty of Agriculture and Forestry, University of Helsinki,
904 2011.

905 Karjalainen, T., Rossi, P., Ala-aho, P., Eskelinen, R., Reinikainen, K., Kløve, B., Pulido-
906 Velazquez, M. and Yang, H.: A decision analysis framework for stakeholder involvement and
907 learning in groundwater management., Hydrol. Earth Syst. Sci. Discuss., 10, 8747-8780,
908 doi:10.5194/hessd-10-8747-2013, 2013.

909 Keese, K. E., Scanlon, B. R. and Reedy, R. C.: Assessing controls on diffuse groundwater
910 recharge using unsaturated flow modeling, Water Resour. Res., 41, W06010,
911 doi:10.1029/2004WR003841, 2005.

912 Kelliher, F. M., Leuning, R. and Schulze, E. D.: Evaporation and canopy characteristics of
913 coniferous forests and grasslands, Oecologia, 95, 153-163, 1993.

914 Kelliher, F. M., Lloyd, J., Arneth, A., Byers, J. N., McSeveny, T. M., Milukova, I., Grigoriev,
915 S., Panfyorov, M., Sogatchev, A., Varlargin, A., Ziegler, W., Bauer, G. and Schulze, E. -.:
916 Evaporation from a central Siberian pine forest, J. Hydrol., 205, 279-296,
917 doi:10.1016/S0022-1694(98)00082-1, 1998.

918 Kløve, B., Ala-aho, P., Bertrand, G., Boukalova, Z., Ertürk, A., Goldscheider, N., Ilmonen, J.,
919 Karakaya, N., Kupfersberger, H., Kvœrner, J., Lundberg, A., Mileusnić, M., Moszczynska,
920 A., Muotka, T., Preda, E., Rossi, P., Siergieiev, D., Šimek, J., Wachniew, P., Angheluta, V.
921 and Widerlund, A.: Groundwater dependent ecosystems. Part I: Hydroecological status and
922 trends, Environ. Sci. & Policy, 14, 770-781, doi:10.1016/j.envsci.2011.04.002, 2011.

923 Koivusalo, H., Ahti, E., Laurén, A., Kokkonen, T., Karvonen, T., Nevalainen, R. and Finér,
924 L.: Impacts of ditch cleaning on hydrological processes in a drained peatland forest,
925 Hydrol. Earth Syst. Sci., 12, 1211-1227, 2008.

926 Koundouri, P., Kougea, E., Stithou, M., Ala-Aho, P., Eskelinen, R., Karjalainen, T. P., Klove,
927 B., Pulido-Velazquez, M., Reinikainen, K. and Rossi, P. M.: The value of scientific
928 information on climate change: a choice experiment on Rokua esker, Finland, Journal of
929 Environmental Economics and Policy, 1, 85-102, 2012.

930 Kumpula, J., Colpaert, A. and Nieminen, M.: Condition, potential recovery rate, and
931 productivity of lichen (Cladonia spp.) ranges in the Finnish reindeer management area, Arctic,
932 152-160, 2000.

933 Kurki, V., Lipponen, A. and Katko, T.: Managed aquifer recharge in community water
934 supply: the Finnish experience and some international comparisons, Water Int., 38, 774-789,
935 2013.

936 Lagergren, F., Lankreijer, H., Kučera, J., Cienciala, E., Mölder, M. and Lindroth, A.:
937 Thinning effects on pine-spruce forest transpiration in central Sweden, For. Ecol. Manage.,
938 255, 2312-2323, 2008.

939 Larson, D. W.: Lichen water relations under drying conditions, New Phytol., 82, 713-731,
940 doi:10.1111/j.1469-8137.1979.tb01666.x, 1979.

941 Lemmelä, R. and Tattari, S.: Infiltration and variation of soil moisture in a sandy aquifer,
942 Geophysica, 22, 59-70, 1986.

943 Lemmelä, R.: Water balance of sandy aquifer at Hyrylä in southern Finland, Ph.D. thesis,
944 University of Turku, Turku, 1990.

945 Lindroth, A.: Canopy Conductance of Coniferous Forests Related to Climate, Water Resour.
946 Res., 21, 297-304, doi:10.1029/WR021i003p00297, 1985.

947 Mustonen, S.: Sovellettu hydrologia, Vesiyhdistys, Helsinki, 1986.

948 National Land Survey of Finland: NLS file service of open data, Laser scanning point cloud
949 (LiDAR), 2012.

950 Odong, J.: Evaluation of empirical formulae for determination of hydraulic conductivity
951 based on grain-size analysis, Journal of American Science, 3, 54-60, 2007.

952 Ohta, T., Hiyama, T., Tanaka, H., Kuwada, T., Maximov, T. C., Ohata, T. and Fukushima, Y.:
953 Seasonal variation in the energy and water exchanges above and below a larch forest in
954 eastern Siberia, Hydrol. Process., 15, 1459-1476, doi:10.1002/hyp.219, 2001.

955 Okkonen, J.: Groundwater and its response to climate variability and change in cold snow
956 dominated regions in Finland: methods and estimations, Ph.D. thesis, University of Oulu,
957 Oulu, Finland, 78 pp., 2011.

958 Okkonen, J. and Kløve, B.: A conceptual and statistical approach for the analysis of climate
959 impact on ground water table fluctuation patterns in cold conditions, J. Hydrol., 388, 1-12,
960 doi:10.1016/j.jhydrol.2010.02.015, 2010.

961 Okkonen, J. and Kløve, B.: A sequential modelling approach to assess groundwater–surface
962 water resources in a snow dominated region of Finland, Journal of Hydrology, 411, 91-107,
963 doi:10.1016/j.jhydrol.2011.09.038, 2011.

964 Rautiainen, M., Heiskanen, J. and Korhonen, L.: Seasonal changes in canopy leaf area index
965 and moDis vegetation products for a boreal forest site in central Finland, Boreal
966 Environ. Res., 17, 72-84, 2012.

967 Repola, J., Ojansuu, R. and Kukkola, M.: Biomass functions for Scots pine, Norway spruce
968 and birch in Finland, Finnish Forest Research Institute (METLA), Helsinki, 28 pp., 2007.

969 Riaño, D., Valladares, F., Condés, S. and Chuvieco, E.: Estimation of leaf area index and
970 covered ground from airborne laser scanner (Lidar) in two contrasting forests, Agric. For.
971 Meteorol., 124, 269-275, 2004.

972 Rodríguez-Caballero, E., Cantón, Y., Chamizo, S., Afana, A. and Solé-Benet, A.: Effects of
973 biological soil crusts on surface roughness and implications for runoff and erosion,
974 Geomorphology, 145, 81-89, 2012.

975 Rosenberry, D. O., Winter, T. C., Buso, D. C. and Likens, G. E.: Comparison of 15
976 evaporation methods applied to a small mountain lake in the northeastern USA, Journal of
977 Hydrology, 340, 149-166, 2007.

978 Rossi, P. M., Ala-aho, P., Ronkanen, A. and Kløve, B.: Groundwater - surface water
979 interacion between an esker aquifer and a drained fen, J. Hydrol, 432-433, 52-60,
980 doi:10.1016/j.jhydrol.2012.02.026, 2012.

981 Rossi, P. M., Ala-aho, P., Doherty, J. and Kløve, B.: Impact of peatland drainage and
982 restoration on esker groundwater resources: modeling future scenarios for management,
983 Hydrogeol. J., 1-15, 2014.

984 Rothacher, J.: Increases in water yield following clear-cut logging in the Pacific Northwest,
985 Water Resour. Res., 6, 653-658, 1970.

986 Scanlon, B. R., Healy, R. and Cook, P.: Choosing appropriate techniques for quantifying
987 groundwater recharge, Hydrogeol. J., 10, 91-109, 2002.

988 Scanlon, B. R., Christman, M., Reedy, R. C., Porro, I., Simunek, J. and Flerchinger, G. N.:
989 Intercode comparisons for simulating water balance of surficial sediments in semiarid regions,
990 Water Resour. Res., 38, 59-1-59-16, doi:10.1029/2001WR001233, 2002.

991 Scibek, J. and Allen, D.: Modeled impacts of predicted climate change on recharge and
992 groundwater levels, Water Resour. Res., 42, W11405, doi:10.1029/2005WR004742, 2006.

993 Shaw, R. H. and Pereira, A. R.: Aerodynamic roughness of a plant canopy: A numerical
994 experiment, Agricultural Meteorology, 26, 51-65, doi:10.1016/0002-1571(82)90057-7, 1982.

995 Smerdon, B., Mendoza, C. and Devito, K.: Influence of subhumid climate and water table
996 depth on groundwater recharge in shallow outwash aquifers, Water Resour. Res., 44,
997 W08427, doi:10.1029/2007WR005950, 2008.

998 Sophocleous, M.: Quantification and regionalization of ground-water recharge in south-
999 central Kansas: integrating field characterization, statistical analysis, and GIS, Spec Issue,
1000 Compass, 75, 101-115, 2000.

1001 Stähli, M., Jansson, P. and Lundin, L. C.: Soil moisture redistribution and infiltration in
1002 frozen sandy soils, Water Resour. Res., 35, 95-103, 1999.

1003 Vesala, T., Suni, T., Rannik, Ü, Keronen, P., Markkanen, T., Sevanto, S., Grönholm, T.,
1004 Smolander, S., Kulmala, M. and Ilvesniemi, H.: Effect of thinning on surface fluxes in a
1005 boreal forest, Global Biogeochem. Cycles, 19, 2005.

1006 Vincke, C. and Thiry, Y.: Water table is a relevant source for water uptake by a Scots pine
1007 (Pinus sylvestris L.) stand: Evidences from continuous evapotranspiration and water table
1008 monitoring, Agric. For. Meteorol., 148, 1419-1432, doi:10.1016/j.agrformet.2008.04.009,
1009 2008.

Wang, Y., Woodcock, C. E., Buermann, W., Stenberg, P., Voipio, P., Smolander, H., Häme, T., Tian, Y., Hu, J., Knyazikhin, Y. and Myneni, R. B.: Evaluation of the MODIS LAI algorithm at a coniferous forest site in Finland, Remote Sens. Environ., 91, 114-127, doi:10.1016/j.rse.2004.02.007, 2004.

Westenbroeck, S. M., Kelson, V. A., Hunt, R. J. and Branbury, K.,R.: A modified Thornthwaite-Mather Soil-Water-Balance code for estimating groundwater recharge, USGS, Reston, Virginia, USA, 2010.

Wierenga, P., Hills, R. and Hudson, D.: The Las Cruces Trench Site: Characterization, Experimental Results, and One-Dimensional Flow Predictions, Water Resour. Res., 27, 2695-2705, 1991.

Winter, T. C., Harvey, J. W., Franke, O. L. and Alley, W. M.: Ground water and surface water; a single resource, USGS, Denver, Colorado, 79 pp., 1998.

Xiao, C., Janssens, I. A., Yuste, J. and Ceulemans, R.: Variation of specific leaf area and upscaling to leaf area index in mature Scots pine, Trees, 20, 304-310, doi:10.1007/s00468-005-0039-x, 2006.

Zaitsoff, O.: Groundwater balance in the Oripää esker, National Board of Waters, Finland, Helsinki, 54-73 pp., 1984.

Zhou, Y.: A critical review of groundwater budget myth, safe yield and sustainability, J. Hydrol., 370, 207-213, doi:10.1016/j.jhydrol.2009.03.009, 2009.

Tables

Table 1. Characteristics of the study site annual climate.

VARIABLE	MEAN	STD
Precipitation [mm]	591	91
Air Temperature [°C]	-0.7	1.1
Reference ET [mm]	426	26

Table 2. Randomly varied parameters, related equations and parameter ranges included in the model runs. For full description of parameters and equations, see Jansson and Karlberg (2004).

Parameter	Part of the model affected	Range	Units	Source
LAI (leaf area index)	Transpiration	0 … 3.5	-	Data, see section 2.1.1
h (canopy height)	Transpiration	5 … 15	m	Data
r_{alai} (increase in aerodynamic resistance with LAI)	Soil evaporation	25 … 75	-	±50% , estimate
r_{Ψ} (soil surface resistance control)	Soil evaporation	100…300	-	±50% approximately to cover the surface resistance reported 150-1000 (Kelliher et al., 1998)
λ_L (pore size distribution index)	Soil evaporation, lichen	0.4 … 1	-	Estimate, to cover an easily drainable range of pressure-saturation curves
Ψ_L (air entry)	Soil evaporation, lichen	1.5 … 20	-	Estimate, to cover a easily drainable range of pressure-saturation curves
θ_L (porosity)	Soil evaporation, lichen	7.5…12.5	%	Data, lichen mean water retention ±SD from samples

$k_{mat,L}$ (matrix saturated hydraulic conductivity)	Soil evaporation, lichen	$5\ 10^4$ … $5\ 10^7$	mm d^{-1}	Estimate, high K values assumed
t_{WD} (coefficient in the soil temperature response function)	Water uptake	10 … 20	-	±50%, estimate
Ψ_c (critical pressure head for water uptake reduction)	Water uptake	200…600	-	±50%, estimate
$k_{mat,S}$ (matrix saturated hydraulic conductivity)	Soil profile	$1.707\ 10^3$…$127.2\ 10^3$	mm d^{-1}	Data from soil sample particle size analysis
k_{minuc} (minimum unsaturated hydraulic conductivity	Soil profile	$1\ 10^{-4}$ …$1\ 10^{-1}$	mm d^{-1}	Estimate k_{mat} * 1E-5
λ_s (pore size distribution index)	Soil profile	0.4 … 1	-	Range to cover measured pressure-saturation curves
Ψ_s (air entry)	Soil profile	20 … 40	-	Range to cover measured pressure-saturation curves
θ_s (porosity)	Soil profile	0.25…0.36	%	Range from soil samples
θ_r (residual water content)	Soil profile	0.01…0.05	%	Range to cover measured pressure-saturation curves

Table 3. Stream baseflow estimates compared to simulated recharge outputs calculated for different timeperiods

Baseflow for 9-10 February 2010 [mm a^{-1}]	Long term average recharge [mm a^{-1}]	Recharge for preceding year 2009 [mm a^{-1}]	Simulated recharge for 9-10 February 2010
312.7	362.8	421.8 (min)	110.0 (min)
		439.5 (max)	135.8 (max)

Table 4. Kendall correlation coefficient for simulation parameters and average annual sum of simulation output variables. ET = evapotranspiration, E = evaporation, for other symbols see Table 2.

Parameter	Total ET	Transpiration	Soil E	Snow E	Infiltration
LAI	0.59*	0.84*	-0.73*	-0.37*	0.18*
h	0.59*	0.84*	-0.73*	-0.37*	0.18*
r_{Ψ}	-0.11*	-0.03	-0.03	-0.61*	0.58*
r_{alai}	-0.13*	-0.02	-0.11*	0.03	-0.05
λ_L	-0.09*	-0.01	-0.11*	0.01	-0.03
Ψ_L	0.01	-0.04	0.11*	-0.04	0.06
θ_L	0.06	0.03	0.01	-0.00	0.09*
$k_{mat,L}$	-0.01	0.02	-0.04	-0.00	-0.00
$k_{mat,S}$	-0.10*	-0.04	-0.07*	0.02	0.01
k_{minuc}	-0.10*	-0.04	-0.07*	0.02	0.01
t_{WD}	-0.05	-0.02	-0.03	-0.05	0.03
Ψ_c	0.18*	0.12*	-0.02	-0.04	0.05
λ_s	0.13*	0.06	0.06	-0.00	-0.23*
Ψ_s	-0.11*	-0.05	-0.04	-0.05	0.04
θ_s	0.02	-0.01	0.03	0.10*	-0.18*
θ_r	0.07*	0.05	-0.01	0.01	0.16*

*Significant correlation, $p<0.05$

Figures

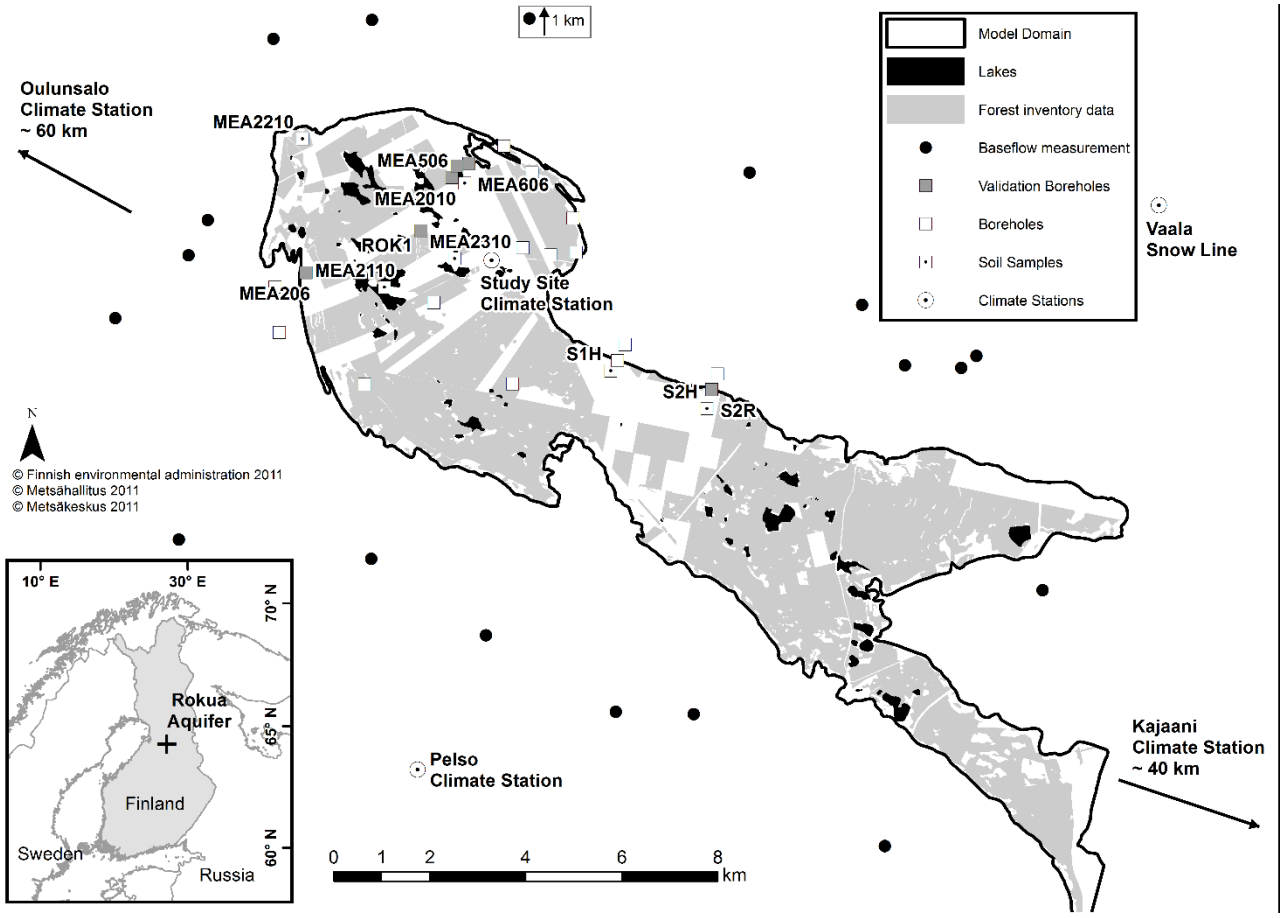

Figure 1. Recharge area of the Rokua esker aquifer. Boreholes in the area were used for model validation and soil type characterization. Baseflow was measured from streams originating outside the groundwater recharge area.

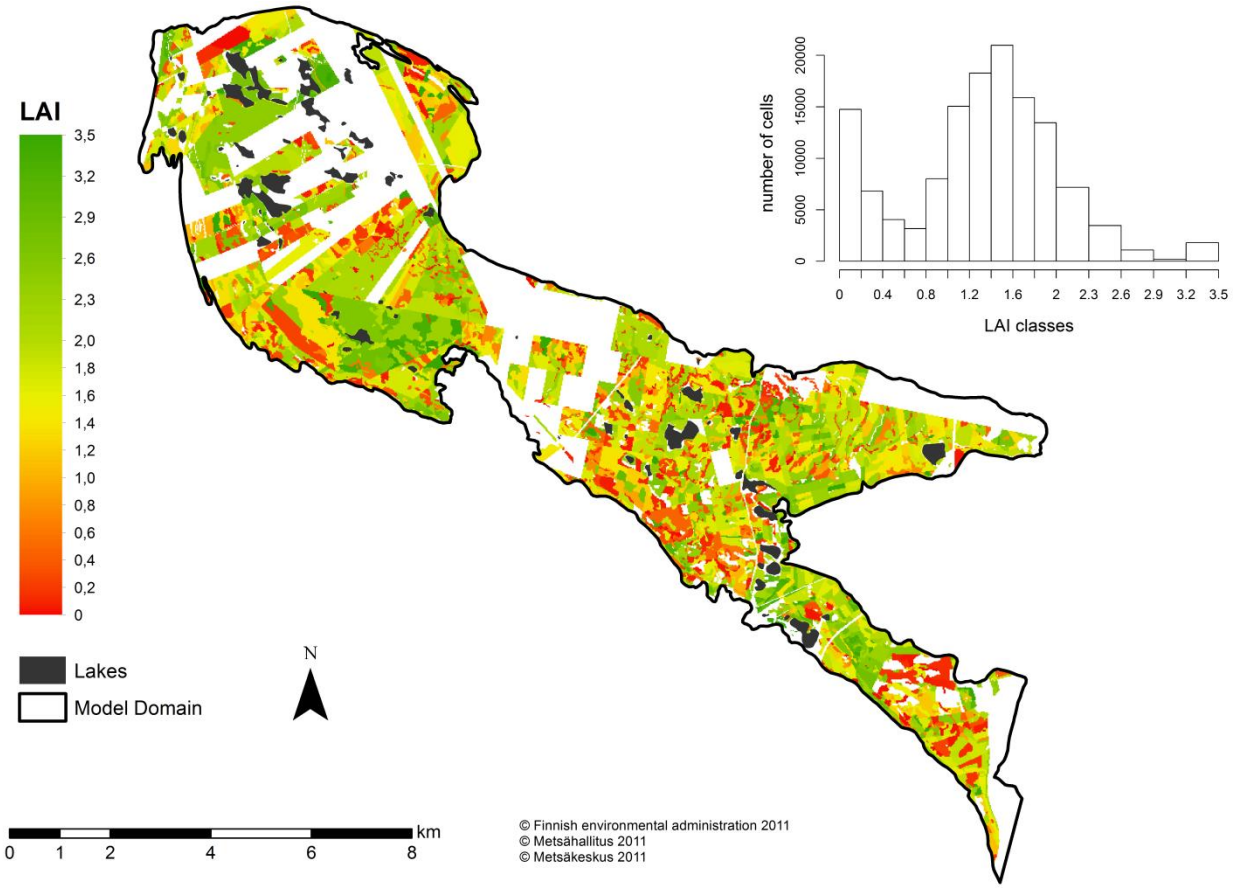

1062

1063 **Figure 2.** Spatial distribution of leaf area index (LAI) and a 20m x 20m cell-based histogram
1064 of LAI values. In areas where forestry inventory data were lacking, a weighted average value
1065 of 1.25 was used in simulations.

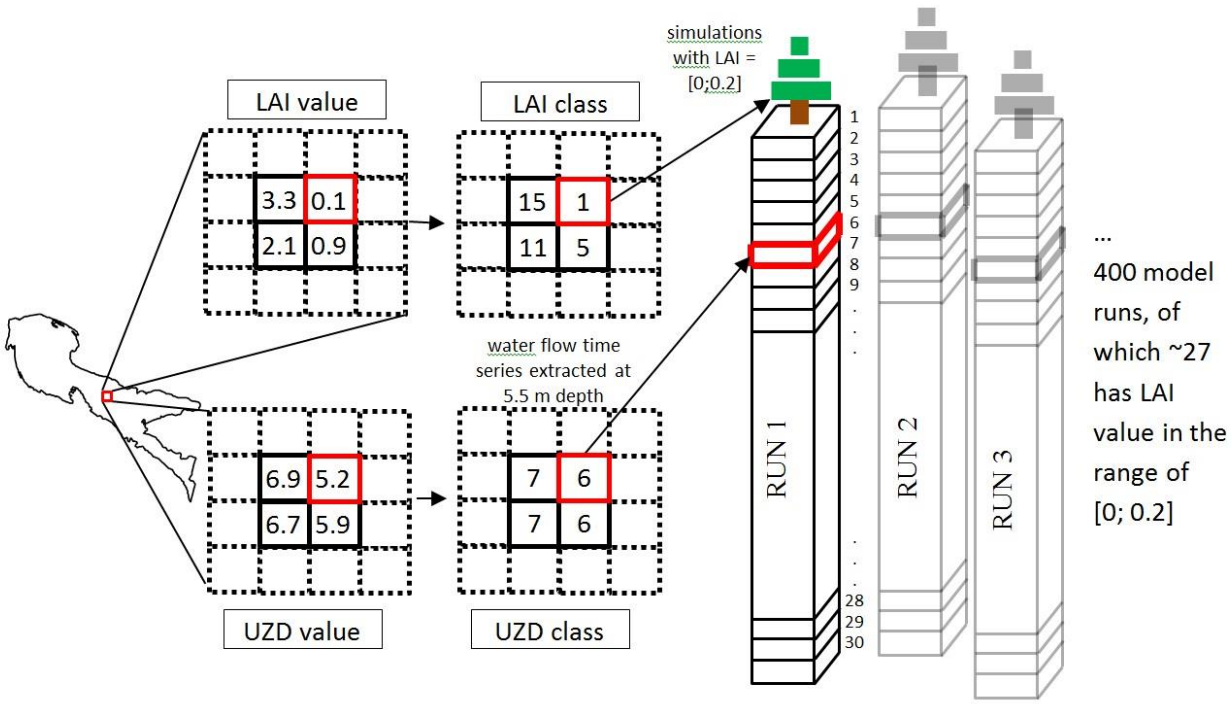

1066

1067 **Figure 3.** Example of selection of water flow simulation data for a random cell in the model
1068 domain for which LAI = 0.1 and UZD = 5.2 m.

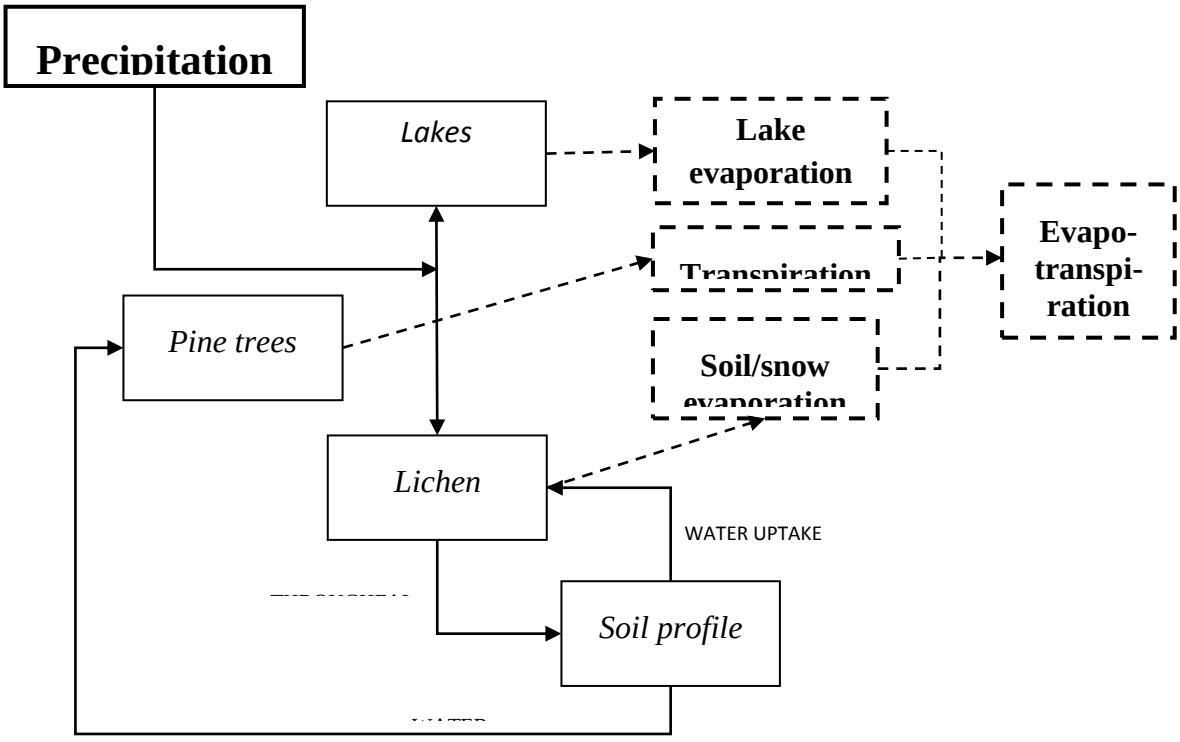

1069

1070 **Figure 4.** Flow chart of different evaporation processes considered in the study.

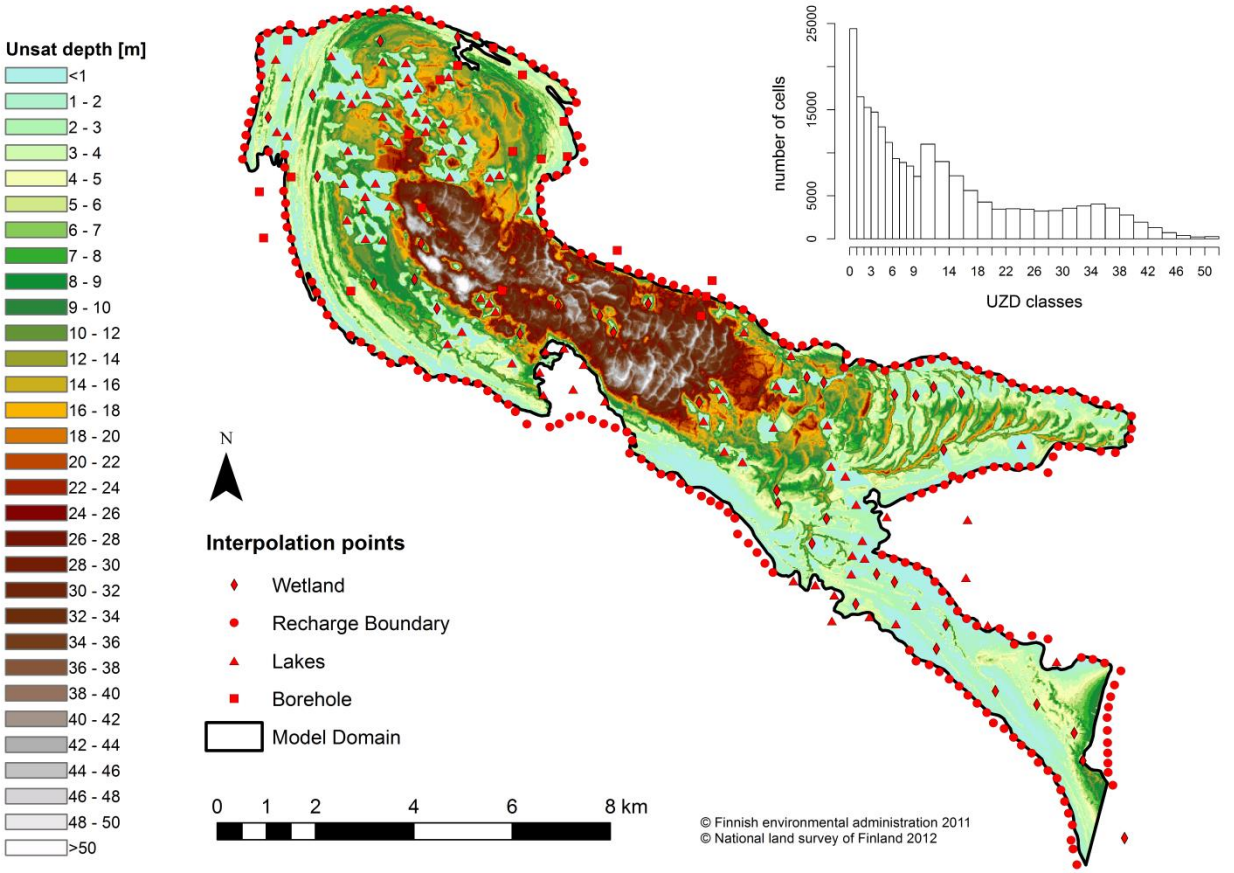

Figure 5. Estimated depth of the unsaturated zone in the model area and interpolation points for estimation of water table elevation.

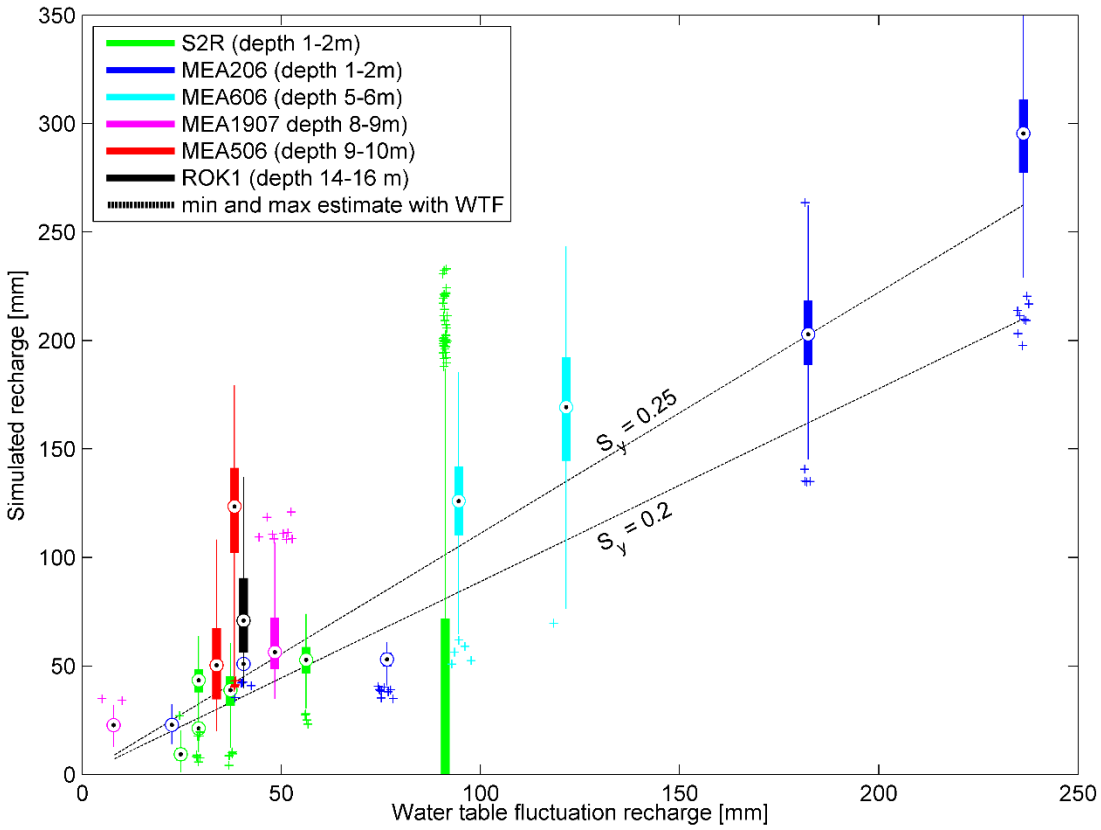

1074

1075 **Figure 6.** Assemblage of simulated recharge for individual recharge events, shown as
1076 boxplots where circles represent the median, bold lines 25-75th percentiles of the simulations,
1077 thin lines the remaining upper and lower 25th percentiles and crosses are outliers. The location
1078 of the boxplots on the x-axis is the WTF estimate for a given recharge event using a specific
1079 yield value of 0.225. The dashed lines indicate the uncertainty in the WTF estimates caused
1080 by the selection of specific yield. The two estimates would agree perfectly (given the
1081 uncertainty in S_y) if all simulations shown as boxplots fell between the dashed lines.

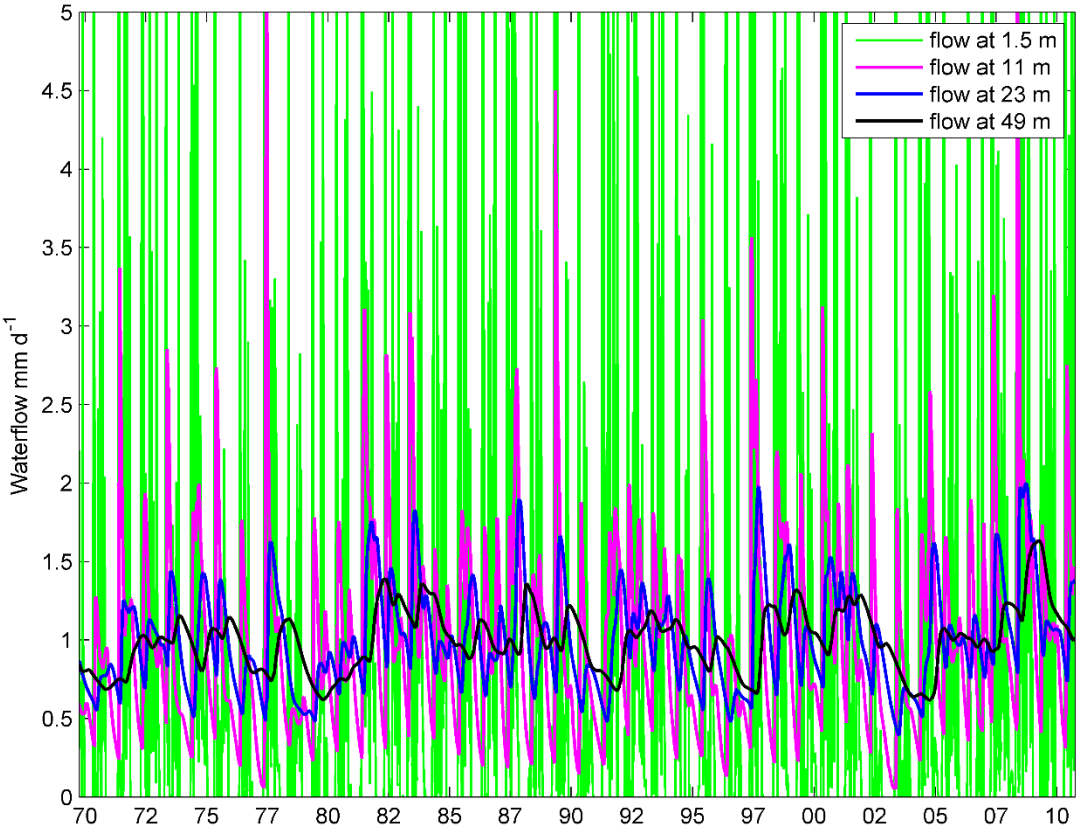

Figure 7. Average water flow outputs at different soil profile depths with LAI range [1.2 … 1.4]. Y-axis is limited to 5 mm d^{-1} to highlight the flow dynamics in the deeper layers, even though peak signal at 1.5 m reaches a value of several cm annually.

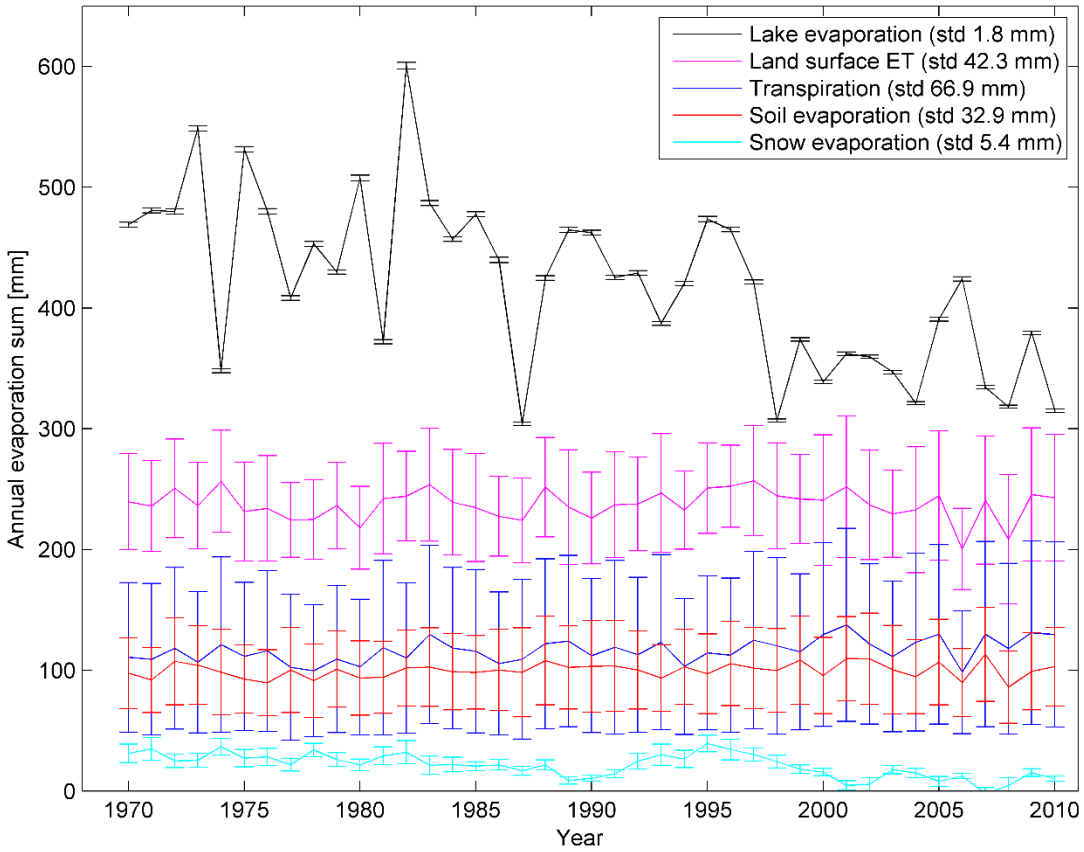

1086

1087 **Figure 8.** Values of different evapotranspiration (ET) components (mean and standard
1088 deviation) simulated for the study period.

1089

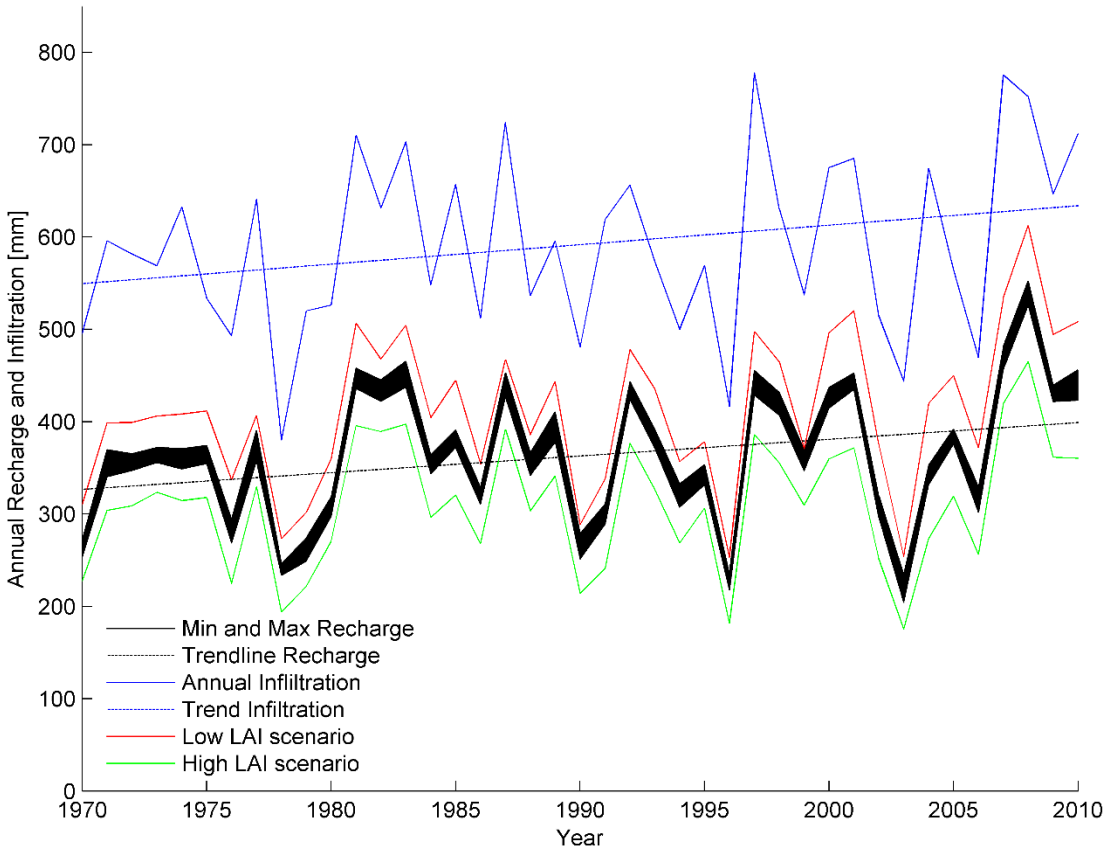

1090

1091 **Figure 9.** Annual recharge time series from simulations where the black area covers the and
1092 minimum and maximum values for different recharge samples. The annual recharge pattern
1093 closely followed trends in infiltration. Effects of different land use management practices over
1094 time on annual recharge rates are shown as high and low leaf area index (LAI) scenarios.

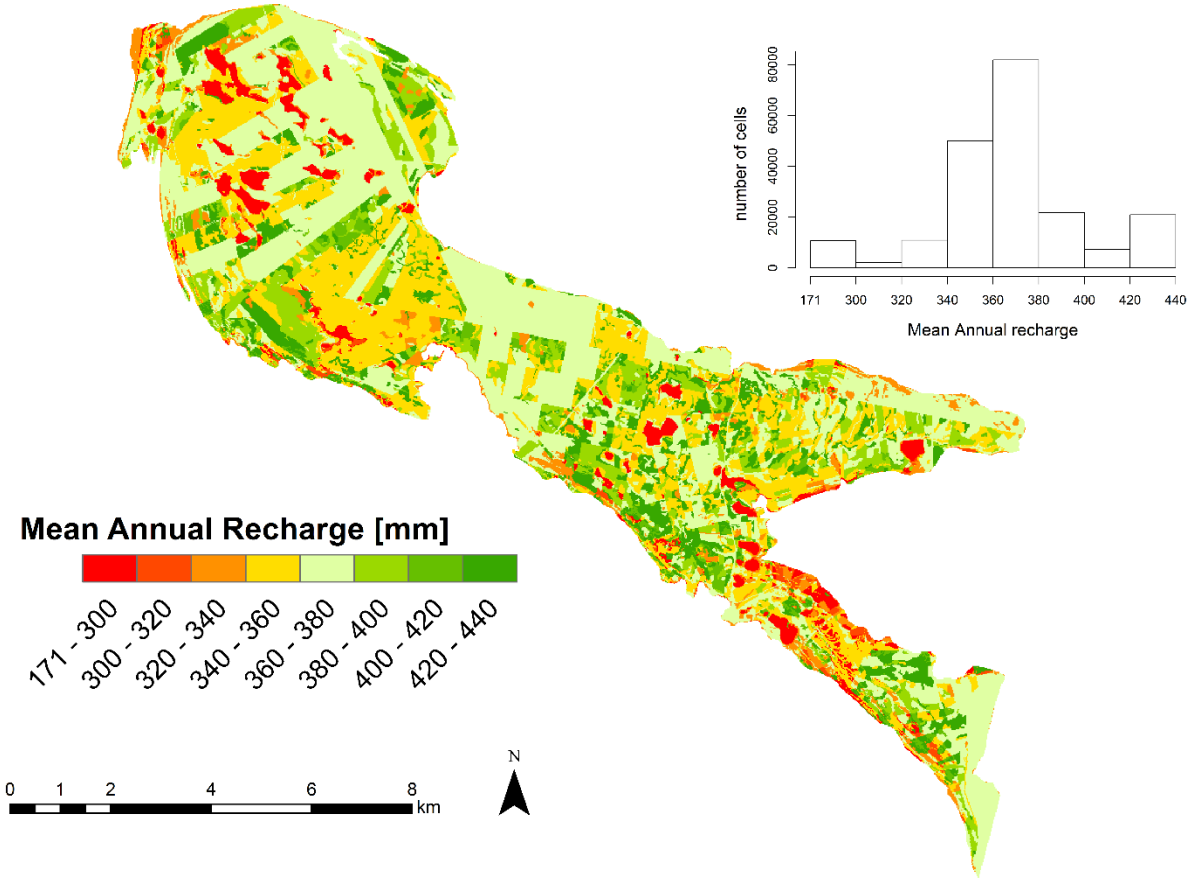

1095

1096 **Figure 10.** Spatial distribution of mean annual recharge, which was influenced mainly by the
1097 Scots pine canopy (LAI), the presence of lakes and, to some extent, areas with a shallow
1098 water table.

1099

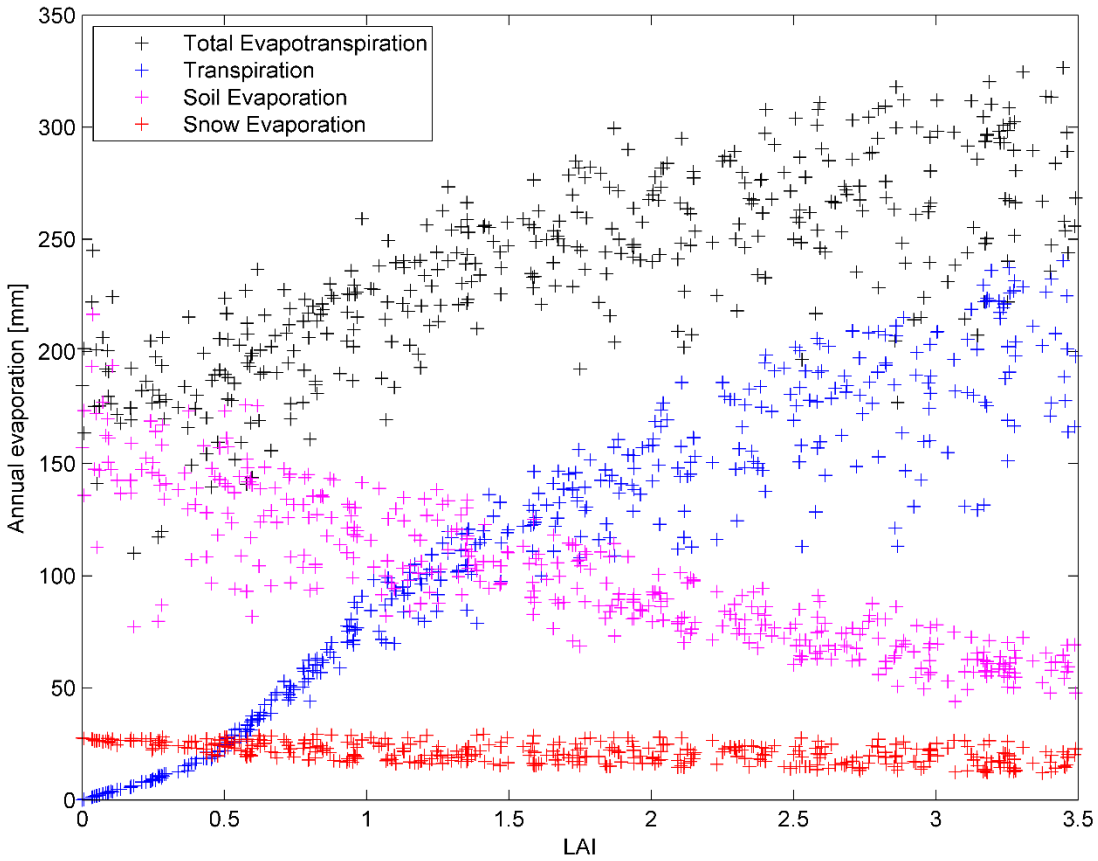

1100

1101 **Figure 11.** Example of scatter plots with the mean annual ET components are plotted as a
1102 function of the variable leaf area index (LAI), showing clear dependence of all ET
1103 components on LAI.